New Fire Protection Materials

Andre L. Thompson

1 Fire Barriers

1.1 Background

Fires involving residential upholstered continue to be the leading cause of civilian fire deaths in the United States [1]. Fire statistics reported by the National Fire Protection Agency (NFPA) between 2013 and 2017 indicates that residential fires in which a RUF item was first ignited caused an estimated annual average of $243 million in direct sources in deadly fires, where RUF is the first item ignited; they account for 55% of home fire deaths [2, 3]. According to the NFPA [2], the vast majority of fire deaths (about 95%) occur when fire spreads beyond the first item ignited (i.e., the upholstery furniture item) and about two-thirds occur when fire spreads beyond the room of origin; which can only be explained by the presence of flaming [4].

There are two alternative ways to decrease RUF flammability risk: (a) by flame prevention (i.e., reducing the probability that flaming will occur by increasing the flaming or smoldering ignition resistance of the item) or (b) by flame mitigation (i.e., limiting the consequences of a burning item, such as flashover, by reducing fire growth) [3]. To enhance ignition resistance in the presence of smoldering ignition sources, tests like Upholstered Furniture Action Council (UFAC) methodology, ASTM E1353, NFPA 260 and California Technical Bulletin 117 2013 (TB 117–2013) [5–8], have been adopted. TB 117–2013 has been adopted as a federal regulation in 2021 [9], and compliance can be met without using chemical fire retardants (FRs) [10].

A. L. Thompson (✉)
Fire Research Division, Engineering Laboratory, National Institute of Standards and Technology, Gaithersburg 20899, USA
e-mail: andre.thompson@nist.gov

X. Huang and W. C. Tam (eds.), *Intelligent Building Fire Safety and Smart Firefighting*, Digital Innovations in Architecture, Engineering and Construction,
https://doi.org/10.1007/978-3-031-48161-1_9

In the past few decades, FRs chemicals have been largely used in attempt to reduce RUF flammability; however, concerns about possible harmful effects on human health and the environment, posed by specific FRs, led to public backlash and a reassessment of costs/benefits associated with the use of such chemicals [11–15]. In 2017, the state of Maine (LD 182) banned any chemical compound for which "fire-retardant" appears on the material safety data sheet [16]. In 2018, California passed a law (AB2998) that banned halogenated, organo-phosphorous, organo-nitrogen chemicals, and nanofillers [17]. At the federal level, the Consumer Product Safety Commission recommended refraining from intentionally adding hazardous additives such as nonpolymeric organo-halogen FRs and has an ongoing project to evaluate additive organo-halogenated flame retardants [15, 18].

Due to the extreme limitations in the use of FRs, fire safety researchers have been looking for alternative approaches to improve fire safety [19]. In this regard, fire barriers, i.e., protective layers designed to separate the flame from a combustible substrate to limit its flame involvement, offer a potential solution. In the context of RUF, fire barriers are usually fabrics placed between the padding materials, like flexible polyurethane foam (FPUF) or polyester fiber fill, and the cover fabric. Barriers have been shown to mitigate the RUF fire hazard by reducing the fire growth and limiting the fire size [20–32].

Passive barriers operate by physical mechanisms of action including heat/mass transfer reduction, endothermic decomposition and dilution effects associated with the release of non-flammable gases (e.g., water vapor) during the decomposition of the barrier [31, 33]. Active barriers operate by both physical and chemical mechanisms. Chemical mechanisms include flame quenching in the gas phase and charring in the condensed phase. Passive barriers adopt fire resistant fibers (e.g., glass, carbon, polysilicic acid/rayon fibers); active barriers use combinations of fibers and/or coatings with gas-phase-active flame retardants for flame inhibition [34]. Because active barriers might be subject to restrictions in RUF depending on the type of fire retardant they adopt, research at NIST is mainly focused on passive barriers.

This chapter has several aims: (a) review the performance of fire barriers in reduced scale "cube test" design and the importance of the wetting point for the prediction of full-scale performance [31] (b) review the effect of mass transfer of liquid products through the bottom of a burning chair to better understand the key parameters affecting the performance and failure of barriers at a full scale [29] (c) review to what extent passive barriers (expected to comply with the aforementioned US State regulations because they do not contain FRs) can delay the fire growth of RUF when exposed to a strong (18 kW) ignition source (equivalent to five sheets of crumpled newsprint) [29] (d) review how the failure mechanism of barrier fabrics in chair mock-up experiments also applies to commercial RUF in furnished compartments, so the use of the cube test can be possibly extended to predict the performance of barrier fabric in realistic fire scenarios [30, 32] (e) demonstrate how new fire protection materials delay fire growth allowing more time for safe egress and allows more time for first responders to intervene and prevent flashover.

1.2 Materials, Density, and Air Permeability

The fire barriers used throughout this chapter will be a combination of one cover fabric (C0) and six barriers (B1 to B6) used in two previous studies [29, 31]. Barriers were selected from commercial fabrics known to be inherently flame resistant [36] and did not contain any halogenated, organo-phosphorous, organo-nitrogen, or nanoparticle-based flame retardants according to the manufacturers', thus, were expected to be compliant with California Assembly Bill 2998 [17]. The selected fabrics were intended to represent—as much as possible and within the number of barriers tested—a variety of commercially available products (nonwoven/woven, thermally thin/thick, high/low air permeability) and a broad range of materials including cellulosic fibers, E-glass fibers [37], para-aramid fibers [38], polysilicic acid fibers [34, 39], oxidized polyacrylonitrile fibers [40], and combinations thereof. Figure 1 shows photos of representative 2 cm wide strips of each fabric. The air permeabilities of each fabric was measured in accordance to the ASTM D737-18 [41]. A breakdown of the fabrics' composition, areal density, and air permeability are summarized in Thompson et al. [29].

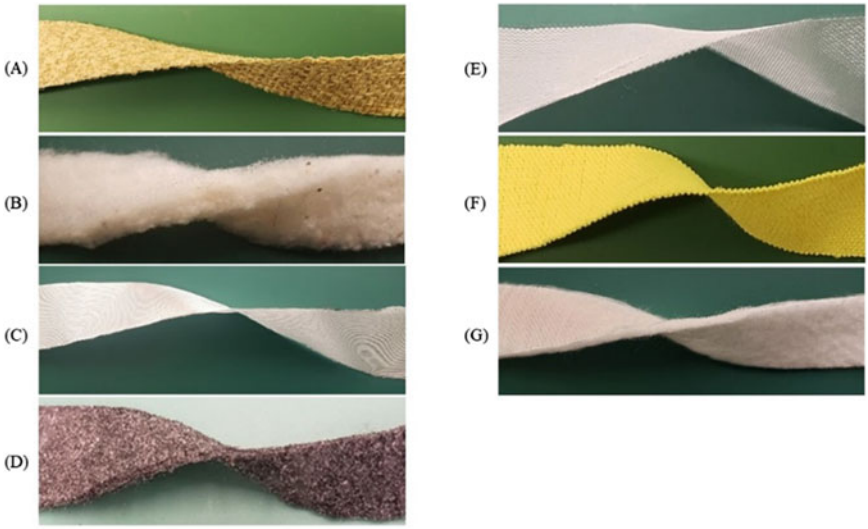

Fig. 1 Pictures showing a 2 cm wide strip sample of: **a**, cover fabric C0; **b** barrier B1, **c** barrier B2; **d** barrier B3; **e** barrier B4; **f** barrier B5; and **g** barrier B6 [29]

1.3 Chemical Analysis of Barriers and Cover Fabric

An elemental analysis of all fabrics was performed by independent laboratories according to the following techniques: ion chromatography (IC) for chlorine (Cl) [42]; the Kjeldahl method [43] for nitrogen (N); inductively coupled plasma atomic emission spectroscopy (ICP-AES) for boron (B), bromine (Br), phosphorus (P), sulfur (S), antimony (Sb), and silicon (Si) according to ASTM E1479-16 [44]; and X-ray fluorescence (XRF) spectroscopy [45] for semi-quantitative screening of antimony, bromine, chlorine, and phosphorus.

The presence of commonly used chlorinated, brominated, and organo-phosphorus FRs was investigated in all fabrics by organic solvent extraction and gas chromatography-mass spectrometry (GC–MS) analysis [46] of the extracted solution. FRs tested for by GC–MS analysis were tributyl phosphate (TBP), tri(2-chloroethyl) phosphate (TCEP), tris(2-chloroisopropyl) phosphate (TCPP), tris(1,3-dichloroisopropyl) phosphate (TDCPP), triphenyl phosphate (TPP), and 1, 2, 5, 6, 9, and 10-hexabromocyclododecane (HBCD). Additionally, B1 was independently tested by aqueous extraction followed by inductively coupled plasma optical emission spectroscopy (ICP-OES) [47] to rule out the presence of boron-based FRs in the inner layer (IL). Details about sample preparation are reported in Data S1 of Thompson et al. [29].

According to manufacturers' specifications, the barriers used in this study did not contain FRs based on halogenated, organo-phosphorous, organo-nitrogen chemical, or nanoparticles, thus they were expected to be compliant with California Assembly Bill 2998 [17]. The barriers were screened for: (a) the presence of elements, which are typically used in FRs, by XRF, IC, Kjeldahl method, ICP-OES, and ICP-AES, and (b) the presence of a number of FRs by GC–MS [48]. This screening methodology for FRs is summarized in Fig. 2 and the results of the screening methodology are summarized in Thompson et al. [29]. For barriers with a bilayer structure like B1 and B6, certain analyses were run on the outer layer (OL) and IL separately.

A full detailed breakdown on the chemical analysis results of each fire barrier and cover fabric is explained in Thompson et al. [29]. To summarize, XRF detected significant amount of P on B (OL and IL) and B6 (OL), but according to Petreas et al. [48], XRF is not reliable screening method for P, and, even for concentrations above 50 (μg/g), caution is recommended when interpreting XRF measurements for P. XRF analysis for Sb, which is considered reliable for concentrations above 40 μg/g [48], revealed Sb concentrations below 40 μg/g for all fabrics. Eventhough XRF detected Cl concentrations, XRF may not be a reliable indicator of chlorinated FRs as both false positive and false negative have been reported [48, 49] and other elemental analysis for Cl are preferable [50, 51].

The Kjeldahl method revealed N with B3 and B5 having the two highest concentrations of ≈180 000 and ≈70 000 μg/g, respectively. Since the Kjeldahl method [43] is applicable to amines, amides, amino acids, and their derivatives (all organonitrogen compounds), organo-nitrogen molecules are present in B3 and B5.

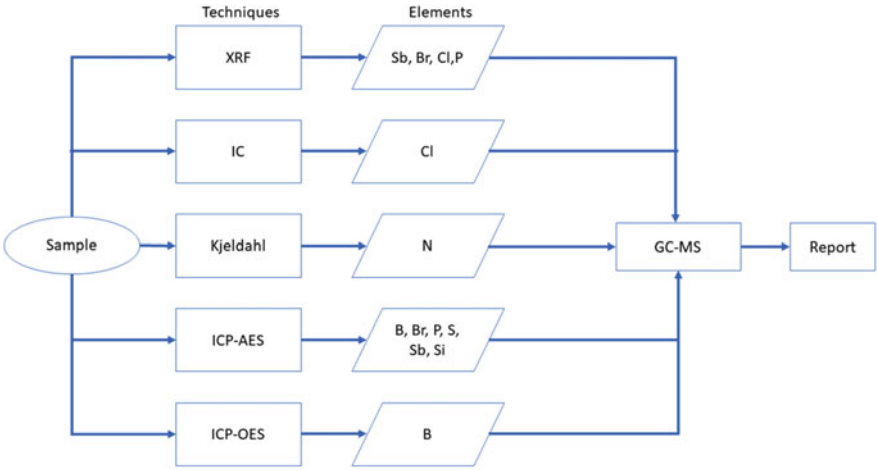

Fig. 2 Diagram illustrating the screening methodology for fire retardants [29]

ICP-AES indicated a significant content of B in B1, B2, B5, and B6 with concentrations ranging from ≈3700 to ≈21 000 μg/g. B2, B5, and B6 contain glass fibers, so B detection in these barriers was likely due to the presence of borosilicate glass [52–54]. B1 contains polysilicic acid and cotton but no glass according to the manufacturer specifications, and B detection (≈3700 μg/g) in this barrier could be associated with the use of additives such as B-based FRs, which are commonly used in combination with cotton [55]. ICP-AES is a more reliable technique to detect P elements than XRF as ICP-AES is very suitable in screening and quantification of P compounds in low concentrations [56]. ICP-OES did not reveal a significant boron content in B1IL (<1 μg/g), thus, the use of B-based FRs in B1IL was ruled out.

GC–MS was used to exclude the presence of some of the most used halogenated and phosphorus-based FRs. In particular, GC–MS analysis did not detect the presence of any of the target FRs. These data support the manufacturer's statement that no FRs were used in the barriers used in this study; however, a more comprehensive investigation based on nontargeted GC–MS [57] or liquid chromatography/time-of-flight mass spectroscopy operated with electrospray ionization [48] would be required to exclude the presence of other FRs that are not included in our list of targeted chemicals.

2 Fire Barriers in Reduced Scale Testing

2.1 Test Instrument/Cube Test Set-Up

This section will investigate the effect of mass transfer of liquid products through burning fire barriers to better understand the key parameters affecting the performance and failure of barriers on a reduced scale "cube test" design and investigate to what extent barriers can delay fire growth of RUF when exposed to a strong ignition source. The instrumentation (cone calorimeter) described in ASTM E1354, was used in all tests. Experiments were run in the cube test configuration [31].

A simplified schematic drawing showing the cube test setup, and an exploded view of the specimen holder and specimen for the Cube test configuration can be viewed in Zammarano et al. [31]. This specimen holder is designed to: (a) create an idealized representative cross-section of the composite product of interest; (b) allow liquid products, generated during pyrolysis, to percolate through the bottom fabrics of the specimen, wet the fire barrier, and form a drip pool that could ignite, and; (c) capture the time at which each of these events occurs. Views with dimensions and materials adopted for the top retainer frame, bottom retainer frame, and liner are provided in Appendix A of Supplemental Information of Zammarano et al. [31].

2.2 Cube Test Specimen Preparation and Procedure

For a detailed description of the cube test specimen preparation and procedure, refer to Zammarano et al. [31]. In summary, one specimen was a control specimen containing the FPUF core, the cover fabric (C0) as top fabric, and no fire barrier. Other specimens using barriers B1 to B6 contained one top fire barrier and one bottom fire barrier (selected among B1 to B6), the cover fabric C0 (above the top fire barrier), and the FPUF core. For a detailed description of the assembly sequence of the specimen refer to Appendix B in Supplemental Information in Zammarano et al. [31].

2.3 Effect of Heat Flux on Burning Behavior

In this test, a 75 kW/m^2 heat flux was adopted because, in full-scale tests on RUF, measured values of flame to surface heat flux exceeding 50 kW/m^2 and reaching up to 100 kW/m^2 have been observed [21, 58]. In addition, in the Cube test, there is no heat source underneath the specimen and the incident heat flux at the bottom of the specimen might not be high enough to support full pyrolysis of the FPUF (low heating rate in FPUF shifts its decomposition toward an oxidative rather than pyrolytic pathway) [59].

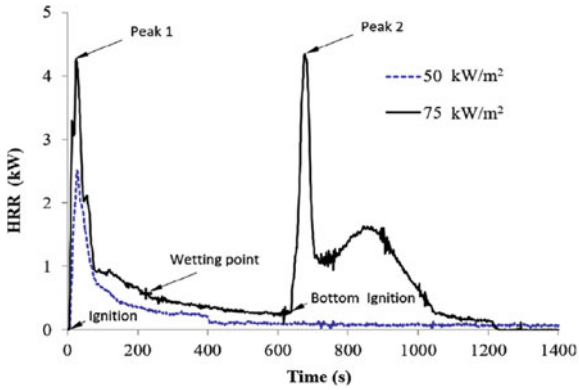

Fig. 3 Heat release rate (HRR) measured for one representative sample with fire barrier B6 at an external heat flux of 50 and 75 kW/m^2 [31]

Figure 3 shows representative HRR curves measured for specimens with barrier B6. In both curves of Fig. 3, the first peak of heat release rate (PHRR) was associated with the combustion of the cover fabric on top of the specimens. The cover fabric (C0) was rapidly consumed during the first peak and, after that, the HRR was mainly due to the combustion of gaseous products produced by foam pyrolysis. At this stage, the FPUF kept collapsing [60] and, thus, the incident heat flux on the FPUF surface and FPUF pyrolysis rate decreased. At 50 kW/m^2, the incident heat flux was not high enough to support flaming. At 75 kW/m^2, flaming was supported throughout the test, and liquid products percolating through the bottom FB became visible within 4 min. A second peak of HRR was observed when the bottom FB (now saturated with liquid products) ignited and, shortly after, flaming drips accumulated in the catch pan and generated a pool fire under the specimen.

Ultimately, at 50 kW/m^2, a significant fraction of the FPUF was converted into char (as typically observed in smoldering combustion) [61] and no liquid products were released under the specimen even after 30 min from test start, whereas at 75 kW/m^2 the FPUF produced visible liquid products underneath the specimen without any significant char production (better mimicking the decomposition pathway observed during the combustion behavior of RUF at full-scale where flaming drips are generated by FPUF) [21] within 4 min from test start.

2.4 Determination of Wetting Point

The presence of liquid products under the specimen at the wetting point is revealed by "wetting" of the bottom FB due to liquid products percolation, or, if no bottom FB is used, by the appearance of liquid products underneath the specimen. The time to "wetting point" is assumed to be a good indicator of the "time to failure" of the fire barrier in the Cube test since, in presence of an ignition source underneath the specimen, the liquid products would readily ignite and likely cause a large increase in HRR.

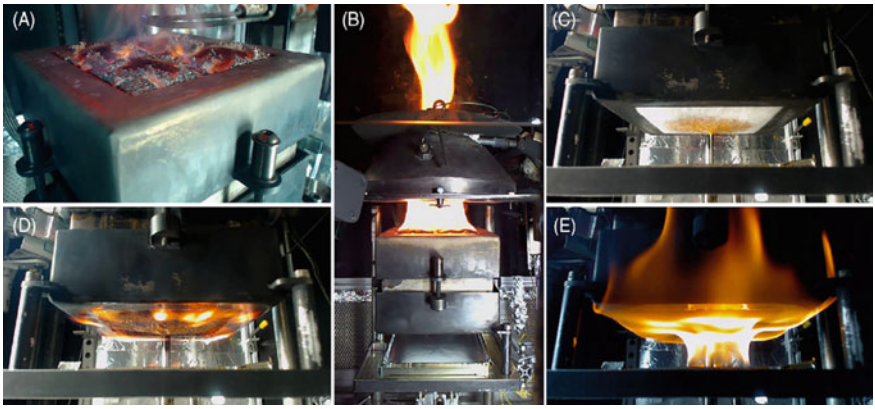

Fig. 4 Snapshots of a representative sample (FB B6 at 75 kW/m^2) displaying the characteristic stages of combustion in the Cube test: **a** ignition; **b** first peak of heat release rate; **c** about 50 s after wetting point; **d** bottom ignition, and **e** second peak of heat release rate [31]

In Fig. 9.2.1, the arrows on the 75 kW/m^2 heat release curve indicate the occurrence of ignition, first peak of heat release rate (peak 1), wetting point, bottom ignition, and second peak of heat release rate (peak 2). Snapshots displaying these characteristic stages of combustion for a representative sample with FB B6 in the Cube test are shown at time of ignition, time of first peak of heat release rate, about 50 s after time of wetting point, time of bottom ignition, and time of second peak of heat release rate (Fig. 4).

Heat release rate curses measured in the cube test for one representative sample are reported in Fig. 5. For each specimen, A reduced cone-calorimetry data are reported in Table 1. For the full table showing all conventional cone-calorimetry data, refer to Zammarano et al. [31]. Compared to C0, specimens containing FBs showed average increases of ≈1.6-fold in time of ignition, up to ≈1.9-fold in time to peak 1, up to ≈1.5-fold in $PHRR_1$, and an average decrease of ≈ threefold in $PHRR_2$, ≈1.3-fold in EHC and ≈1.2-fold in THR.

The significant reduction in EHC, induced by FBs, was not due to a free-radical trapping mechanism (FBs did not contain significant amounts of gas-phase FRs) but likely to the release of gaseous pyrolyzates through the bottom FB, where they did not burn for $t_w < t < t_{BI}$ (video recordings show that visible smoke—and presumably gas products—were released underneath the specimen starting at $t \approx t_w$ and that the smoke release rate visibly increased until $t \approx t_{BI}$), and possible flame quenching over the FB [62]. This fire scenario is not unrealistic and has been observed in full-scale RUF tests before the bottom of the item ignites [29]. The time required for the appearance of flaming on the bottom of the specimen, t_{BI}, ranged from an average value of 106 s to 658 s (for C0s and B6, respectively).

The PHRR is highly dependent on a multitude of factors related to liquid products' flaming (such as flow, release timing and release location of liquid products, type of substrate under the item, substrate-to-item distance, extent of feedback between

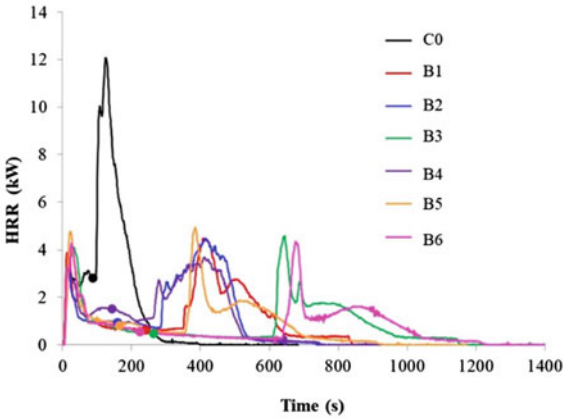

Fig. 5 Heat release rate (HRR) curves measured in the Cube test for one representative sample, cover fabric only sample, C0, and samples with barriers B1 to B6 at an external heat flux of 75 kW/m^2. For each curve, the circled data point indicates the wetting point [31]

pool-fire, residual item, etc.) [63] that even achieving a good experimental reproducibility for PHRR at full-scale may be challenging, and achieving a robust full-scale PHRR prediction by the only means of a reduced-scale test may be unfeasible. However, a conceptual analysis of the burning behavior of RUF (or cored composites in general) can highlight key stages of full-scale fire development and, as presented in Zammarano et al. [31, 32], it is apparent that the wetting point measured in the Cube test may be a valuable metric to predict the performance of fire barriers in RUF and how they can impact the transition between these stages.

3 Fire Barriers in Full-Scale Testing: Chair Mock-Ups

3.1 Chair Mock-Ups

This section has two aims: (a) to further investigate the effect of mass transfer of liquid products through the bottom of a burning chair to better understand the key parameters affecting the performance and failure of barriers at a full scale and (b) to investigate to what extent passive barriers (expected to comply with the aforementioned US State regulations because they do not contain FRs) can delay the fire growth of RUF when exposed to a strong (18 kW) ignition source (equivalent to five sheets of crumpled newsprint) [58].

A chair mock-up was composed of four cushions: a seat cushion, a back cushion, and two armrest cushions. Details about the dimensions of the cover fabric and chair construction can be found in Thompson et al. [29]. The control chair mock-ups (chair C0) included only the cover fabric C0, whereas all other chairs (chair B1 to B6) added a barrier (B1 to B6) as an interliner between the cover fabric and the padding material. Metal staples were used to close the barrier seam because seam failure was previously observed with polyamide threads [23], aluminum zippers held

Table 1 Reduced Cube test data at an external heat flux of 75 kW/m^2. For the full table is Zammarano et al. [31]

	t_{p1} (s)	$PHRR_1$(kW)	t_w (s)	Q_{Cube}(kW)	t_{BI} (s)	t_{P2} (s)	$PHRR_2$(kW)	THR (MJ)	EHC (MJ/Kg)
C0	14 ± 1	3.20 ± 0.10	90 ± 3	2.80 ± 0.10	106 ± 2	118 ± 12	11.5 ± 1.5	1.13 ± 0.02	25.2 ± 0.2
B1	15 ± 3	4.15 ± 0.27	235 ± 17	0.62 ± 0.03	381 ± 49	440 ± 48	4.3 ± 0.3	1.02 ± 0.05	22.1 ± 0.5
B2	16 ± 1	3.32 ± 0.12	153 ± 2	0.96 ± 0.02	278 ± 19	410 ± 24	4.1 ± 0.4	1.05 ± 0.03	23.8 ± 0.6
B3	27 ± 5	4.42 ± 0.25	258 ± 7	0.48 ± 0.02	591 ± 19	620 ± 22	4.7 ± 0.4	0.98 ± 0.02	19.0 ± 6.4
B4	16 ± 1	3.58 ± 0.14	143 ± 2	1.51 ± 0.08	260 ± 8	404 ± 11	3.8 ± 0.2	1.06 ± 0.01	23.9 ± 0.1
B5	21 ± 1	4.68 ± 0.47	164 ± 4	0.90 ± 0.09	354 ± 12	376 ± 12	4.9 ± 0.1	0.99 ± 0.06	23.3 ± 0.2
B6	26 ± 1	4.27 ± 0.13	222 ± 2	0.56 ± 0.06	658 ± 28	694 ± 25	4.4 ± 0.2	1.00 ± 0.05	22.2 ± 1.3

in place by polyamide webbing [22], thermoplastic thread and nylon zippers [21], and polyaramid thread [64].

3.2 Flammability Testing

Tests were conducted at NIST's National Fire Research Laboratory under a 6.1 m by 6.1 m exhaust hood [65]. The average expanded uncertainty (calculated with a coverage factor of 2 corresponding to an approximately 95% confidence interval) [66] for generic combustible fuel was 6.8% in the range from 100 to 3000 kW. The range of expanded uncertainty for the natural gas (fuel consumption) verification burners is 1.4% to 1.8%. Detailed information on the NIST calorimetry measurement system is provided by Bryant and Bundy [65].

Seven chair mock-up combinations (one control chair, chair C0, and six chairs with barriers, chairs B1 to B6) were tested in triplicates for a total of 21 tests; however, due to improper assembly of a B2 chair, only two replicate tests were accepted for B2 chairs. Chairs were assembled on a metal test frame shown in Thompson et al. [29]. Figure 6 shows the test setup used in the flaming tests. A detailed description of the test setup is explained in Thompson et al. [29].

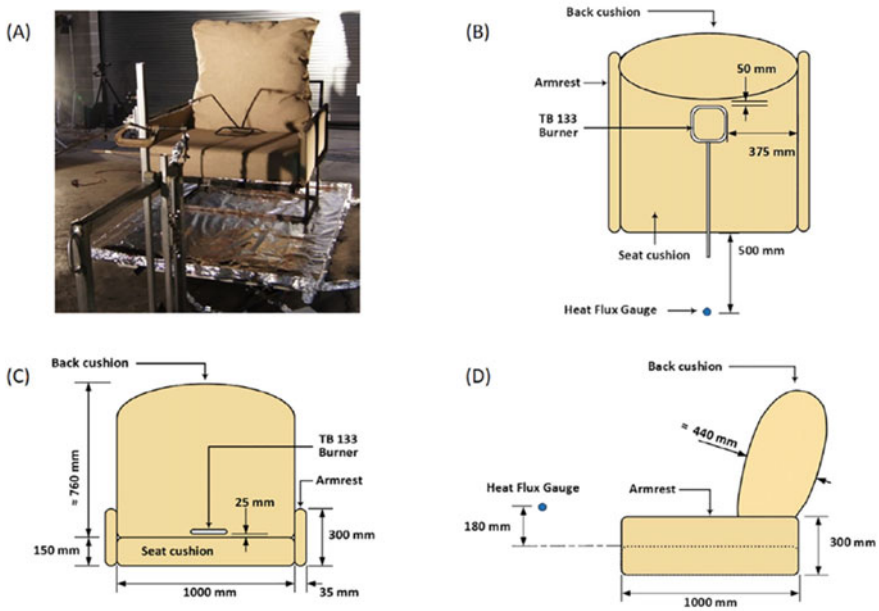

Fig. 6 Test setup used in flaming tests: **a** photo showing a chair mock-up assembled on the metal frame with a burner, heat flux gauge, and catch pan; **b** top view schematic; **c** front view schematic; and **d** side view schematic (nominal dimensions, back cushion not to scale) [29]

3.3 Effects of Barriers on Fire Growth

In order to illustrate the effects of barriers on fire growth in the given test scenario, Fig. 7 shows snapshots for representative chair mock-ups without a barrier and with barrier B6 at t = 30 s, t = 80 s (when the burner was turned off and removed), at the time of pool fire formation, and at the time of peak of heat release rate (PHRR). B6 was the most effective barrier in this study, delaying the intense burning of the chair by at least 20 min.

In a typical test without a barrier, flame jets from the burner simultaneously ignited the top surface of the seat cushion and the front bottom of the back cushion within a few seconds. The polypropylene cover fabric quickly melted and peeled away from the spreading flame front, exposing the padding material which quickly ignited. Shortly after the removal of the burner, the back cushion completely collapsed. Intense flaming over the seat cushion eventually generated a hole in the center of the cushion. Flaming liquid products (mainly, regenerated polyols, produced by the pyrolyzing foam, and possibly liquefied polyester) [35] poured through the hole onto the catch pan and quickly formed a pool fire. Heat flux feedback from the pool fire to the seat cushion increased the generation and release rate of flaming liquid, which in turn produced a larger pool fire and stronger heat flux feedback over the seat cushion and pool fire. This was a self-accelerating process that led to an abrupt increase in heat release rate and continued until the FPUF and regenerated polyol in the seat cushion and the liquid pool were depleted. The peak heat release was reached approximately 1 min from the initial pool fire formation.

Fig. 7 Snapshots for representative chair mock-ups without a barrier (**a** at t = 30 s; **b** at t = 80 s; **c** at t = 2 min 10 s; and **d** at t = 3 min 16 s) and with barrier B6 (**e** at t = 30 s; **f** at t = 80 s; **g** at t = 24 min; and **h** at t = 24 min 48 s) [29]

In a typical test with a barrier, the burner ignited the cover fabric over the seat cushion and along the lower front bottom of the back cushion within a few seconds. The polypropylene cover fabric quickly melted/pyrolyzed along the flame front exposing the barrier, which remained intact and protected the padding material by decreasing the heat transfer from the flames. As a result, the pyrolysis rate of the padding material (hence, the heat release rate and flame size) decreased in the chair with barriers compared to the control chair. While the barrier was still intact, the thermoplastic polyester fiber fill inside the back cushion kept melting and/or pyrolyzing until the back cushion collapsed and tipped forward past the nichrome wire. Afterward, the rapid ignition of the cover fabric on the rear side of the back cushion and the increase in heat flux on the residual polyester fiber fill caused a temporary rise in heat release rate (HRR), which generated a first peak in the heat release rate ($PHRR_1$). Burning continued until an intense flaming appeared underneath the seat cushions, and, shortly after, flaming drips accumulated under the chair, generating a pool fire. The flame size increased until the second, most intense peak of heat release rate ($PHRR_2$) was reached about 1 min after initial pool formation.

Figure 8 shows representative HRR curves measured for the chair mock-ups with barrier (B1-B6) and the control chair mock-up with no barrier (C0). HRR plots for all repeat tests are also shown in Thompson et al. [29]. The control chair reached HRR values above 2500 kW within 3 min. Such rapid fire growth would most likely lead to flashover conditions in most residential fire scenarios [67]. A HRR of 1000 kW generally leads to flashover in a small bedroom and in dwellings where flaming can spread from RUF to other combustible items in the compartment, independent of the room size [68].

In comparison, all barriers significantly decreased the fire growth by generating a HRR plateau between the appearance of a first peak of heat release rate ($PHRR_1$)

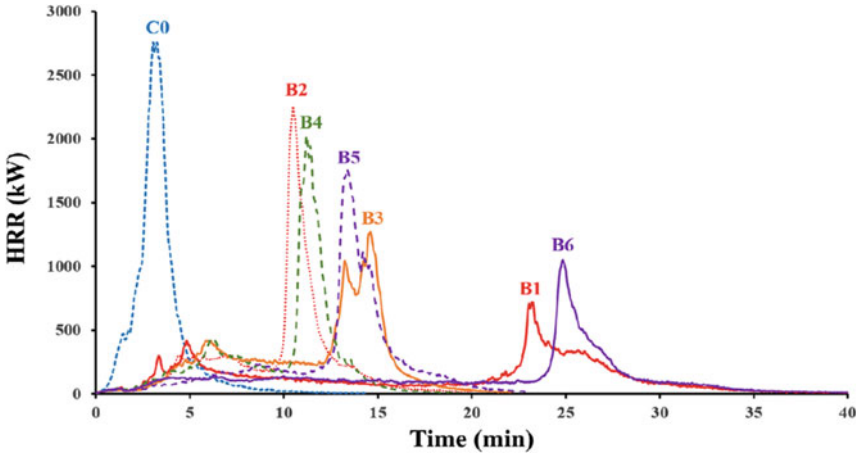

Fig. 8 Representative heat release rate curves for the mock-up chair with no barrier (C0) and the mock-up chairs containing barriers (B1-B6) [29]

and a second, higher peak ($PHRR_2$), which shortly followed the formation of a pool fire. This two-peak burning behavior in RUF and the role of pool fire on burning rate are consistent with previously reported studies [21, 22, 69, 70]. The intensity and timing of $PHRR_2$ are highly dependent on factors related to the flaming of liquid products (such as flow, release timing, and release location of liquid products, type of substrate under the item, substrate-to-item distance, extent of feed-back between pool fire, residual item, etc.) [71].

During the HRR plateaus, the HRR stabilized at roughly constant values that ranged between about 100 and 300 kW and lasted between 9 and 22 min, depending on the barrier. The intensity of $PHRR_1$ was presumably affected by the barrier effectiveness (i.e., extent of heat and mass transfer reduction) and the amount of combustible material (i.e., cover fabric and fiber fill) left in the back cushion when it fell forward past the nichrome wire. B6 chairs took the longest to collapse and no obvious $PHRR_1$ was detected (see Fig. 8). Table 2 shows the values of the flaming characteristics.

Depending on the barrier, time to peak 1 (t_{P1}) varied between 5 and 7 min and $PHRR_1$ between 300 and 400 kW; time to peak 2 (t_{P2}) increased from about 3 min for the control mock-up to about 22 min (≈sevenfold increase) for the mock-ups containing B1 and B6. In all chair mock-ups, $PHRR_2$ was by far the stronger peak, and its average value was reduced in the presence of barriers from about 2600 kW for the control chair to about 900 kW for barriers B1 and B6 (about a threefold decrease). The best barriers also induced a marginal reduction (under 15%) in THR, EHC, and ML, which was presumably due to an increase in the amount of FPUF charring; in fact, the lower the FPUF pyrolysis rate (due to the presence of the barrier), the higher the FPUF char yield [72].

Figure 9 shows heat flux curves for each chair type (the same representative tests are shown in Fig. 8). The flux gauge was positioned about 50 cm from the front of the chair and about 74 cm over the catch pan (see Fig. 6). The time at which heat fluxes of 20 kW/m^2 (t_{HF20}) and 2.5 kW/m^2 ($t_{HF2.5}$) were reached on the flux gauge is summarized in Table 3.

Table 2 Values of t_{p1}, $PHRR_1$, t_{P2}, $PHRR_2$, THR, EHC, and ML and barrier used in each chair mock-up [29]

	t_{P1} (min)	$PHRR_1$ (kW)	t_{p2} (min)	$PHRR_2$ (kW)	THR (MJ)	EHC (MJ/kg)	ML (%)
C0	–	–	3.3 ± 0.2	2610 ± 154	311 ± 5	24.3 ± 0.4	93 ± 3
B1	4.9 ± 0.9	294 ± 78	22.2 ± 2.2	888 ± 157	307 ± 12	22.4 ± 0.3	87 ± 1
B2	4.9 ± 0.6	288 ± 6	11.5 ± 1.4	2025 ± 329	288 ± 8	23.9 ± 0.1	82 ± 2
B3	5.0 ± 0.8	296 ± 46	14.1 ± 0.6	1030 ± 341	328 ± 3	23.7 ± 0.2	87 ± 2
B4	6.6 ± 0.4	392 ± 40	10.9 ± 1.0	1817 ± 222	304 ± 2	24.0 ± 0.2	89 ± 1
B5	7.0 ± 0.5	328 ± 59	12.6 ± 0.6	1648 ± 133	321 ± 3	23.8 ± 0.2	83 ± 1
B6	–	–	22.7 ± 3.4	991 ± 319	297 ± 6	22.2 ± 0.3	83 ± 1

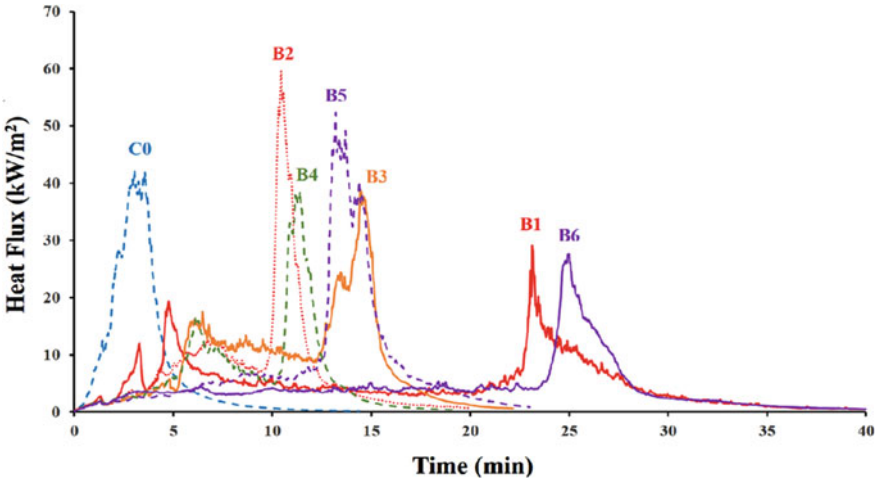

Fig. 9 Representative heat flux curves for each chair type (the same representative tests of Fig. 8 were used) [29]

Table 3 Time to reach heat flux of 2.5 kW/m^2 ($t_{HF2.5}$) or 20 kW/m^2 (t_{HF20}), and peak of heat flux (PHF) with time to PHF (t_{PHF}) [29]

Barrier	$t_{HF2.5}$ (min)	t_{HF20} (min)	PHF (kW/m^2)	t_{PHF} (min)
C0	0.6 ± 0.1	1.8 ± 0.1	53 ± 9	2.9 ± 0.1
B1	2.8 ± 0.7	21.7 ± 2.1	24 ± 5	22.0 ± 2.3
B2	2.7 ± 0.3	10.9 ± 1.3	52 ± 11	11.5 ± 1.5
B3	2.3 ± 0.3	13.3 ± 0.6	34 ± 6	14.1 ± 0.5
B4	1.5 ± 0.6	9.2 ± 2.9	42 ± 5	10.9 ± 0.9
B5	4.0 ± 0.9	12.1 ± 0.6	47 ± 5	12.9 ± 0.3
B6	2.8 ± 0.6	22.6 ± 3.1	29 ± 5	22.8 ± 3.5

Note Uncertainties are reported as ± one experimental SD calculated over three independent observations for each chair type, except chair B2 for which only two independent observations are available

At $t = t_{HF2.5}$, the conditions in proximity of the flux gauge are untenable. Occupants can tolerate a heat flux of 2.5 kW/m^2 for a short amount of time, but such conditions will quickly lead to incapacitation [73]. The value of $t_{HF2.5}$ ranged between a minimum of 0.6 (±0.1) min for chair C0 to a maximum of 4.0 (±0.9) min (almost a sevenfold increase) for B5. Except for incapacitated or immobile individuals that are unlikely to survive unless rescued, people can usually move away from a fire to areas that are tenable and possibly escape. However, untenable conditions will be eventually reached within the entire compartment. In ISO 9705 rooms, this happens when the HRR reaches roughly 400 kW and the hot smoke gas layer descends to about 1.2 m from the floor level [68]. This 400 kW criterion would suggest that

tenable conditions would be maintained in the room until the end of the HRR plateau phase with most barriers (see Fig. 8).

The highest reductions in PHF were achieved with B1 and B6 (roughly twofold reductions compared to the C0 chairs). The reduction in heat flux during the plateau phase is expected to limit the fire growth in a compartment by preventing flame spread to surrounding items. A heat flux of about 20 kW/m^2, which is required for non-piloted flaming ignition, [74–76] was reached in less than 2 min in chair C0 but required over 20 min in chairs with barriers B1 and B6 (see t_{HF20} in Table 3).

3.4 Mechanism of Barrier Failure

All barriers significantly mitigated the fire hazard of the chair mockups by reducing the burning rate as compared to unprotected mockups until the end of the HRR plateau phase, when an abrupt increase in HRR occurred. The phenomena that led to this rapid increase in HRR (referred to as "barrier failure") at the end of the plateau phase is illustrated and discussed below.

Figure 10 shows video snapshots for a representative B6 chair, illustrating the sequence of events that occurred underneath the chair and led to the failure of the barrier. The flaming intensity varied depending on the barrier and was visibly enhanced in proximity of the armrests by heat flux feedback from the vertical surfaces. At this stage, flames were mainly sustained by the gaseous pyrolyzates produced by the padding material in the seat cushion, while the liquid products (mainly regenerated polyols [35]) accumulated inside the barrier envelope on top of the receding FPUF [77]. Eventually, the liquid products, now in contact with the barrier, started percolating through the bottom of the seat cushion.

This process is shown in Fig. 10. In particular, the inset in Fig. 10 highlights an area where the cover fabric has been removed due to melting, flaming, and dripping, and the barrier (normally white) shows brown areas that expanded over time due to liquid products percolating through and wetting the outside of the barrier. When wetting occurred, burning of the cover fabric sustained flaming underneath the chair and generated flaming drops which accumulated under the chair mock-up; meanwhile, smoke began to be released from the bottom of the chair and increased over time (see Fig. 10). The arrows in the Fig. 10 inset indicate regions where wetting occurred.

Eventually, flaming of the cover fabric led to the ignition of liquid products over the wetted areas. Bottom ignition was revealed by sustained flaming on the bottom of the seat cushion in regions where the cover fabric was no longer present (see Fig. 10). The inset in Fig. 10 zooms in on the location where bottom ignition occurred. Bottom ignition gave rise to more intense and prolonged flaming compared to the cover fabric flaming (where the flame front kept moving due to fuel depletion). Bottom ignition was identified by analyzing the videos recorded by the bottom camera for each test.

Bottom ignition led to an increase in incident heat flux over the bottom of the cushion, which in turn led to an increase in barrier degradation and in the pyrolysis rate of residual foam and liquid products; as a result, the percolation rate of liquid products

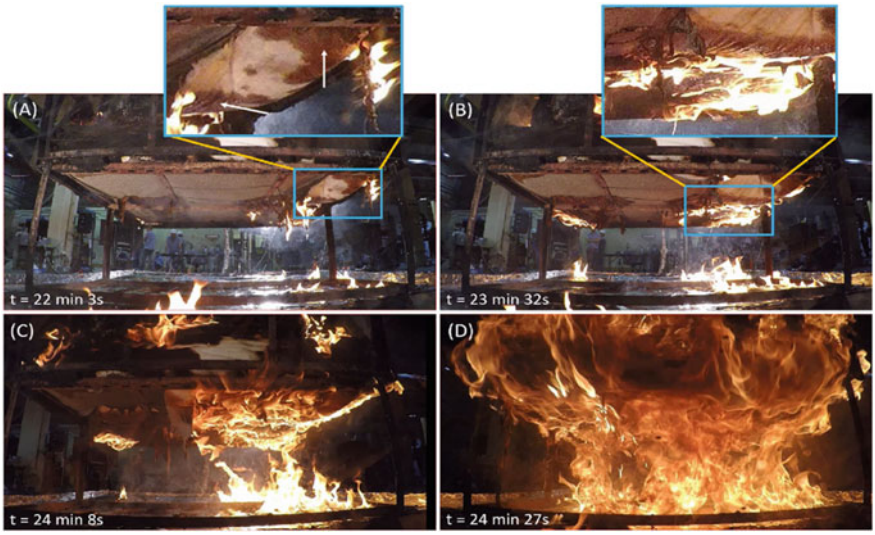

Fig. 10 Video frame grabs for a representative B6 chair mock-up illustrating the sequence of events that led to the failure of barriers; **a** "wetting" of the barrier due to the percolation of liquid products through the barrier; **b** ignition of liquid products ("bottom ignition"); **c** initial pool fire formation; and **d** feedback between the flame on the pool fire and the remaining fuel in the chair mock-up at the time of $PHRR_2$ [29]

increased and more fuel was available to feed flaming underneath the cushion and increase the heat release rate. Hereafter, the amount of liquid products percolating through the barrier exceeded the amount burned at the bottom of the cushion and a liquid pool began to form underneath the mock-up on the support stand. A pool fire was eventually generated (Fig. 10). Noticeably, at this stage, the barrier was still intact, yet the heat release rate kept rapidly increasing—with the self-accelerating feedback mechanism which was previously described until the peak value occurred. For each chair mockup, Table 4 reports bottom ignition characteristics.

For the control chairs C0, bottom ignition coincided with the appearance of flaming underneath the mock-up when liquid products immediately ignited, and flaming liquids started feeding the pool fire; t_{BI} occurred at (2.2 ± 0.1) min when the HRR was about 820 kW; it only took (1.1 ± 0.1) min to reach a $PHRR_2$ of (2610 ± 150) kW from t_{BI}; $AHRR_{BI}$ was (309 ± 35) kW and only (12.9 ± 1.7) % of THR was released by the time bottom ignition occurred (see Table 4). The addition of a barrier substantially delayed bottom ignition. t_{BI} increased from about 2 min for the control chair, to about 20 min for barriers (B1 and B6).

The difference in time, t_{P2}—t_{BI}, was about 2 min for all chairs except chair B4 (which had a t_{P2}—t_{BI} of about 4 min). Hence, barriers were able to moderate the HRR until bottom ignition. After that the HRR increased abruptly and reached its peak value within a couple of minutes. This is a strong indication that the barrier failure was triggered by bottom ignition.

Table 4 Time to bottom ignition (t_{BI}), elapsed time between bottom ignition and $PHRR_2$ (t_{P2}—t_{BI}), heat release rate at bottom ignition (HRR_{BI}), average heat release rate calculated between ignition and bottom ignition ($AHRR_{BI}$), and percentage of THR released between ignition and bottom ignition ($\%THR_{BI}$), as a function of the barrier used in the chair mock-up [29]

Barrier	t_{BI} (min)	t_{P2}—t_{BI} (min)	HRR_{BI} (kW)	$AHRR_{BI}$ (kW)	$\%THR_{BI}$ (%)
C0	2.2 ± 0.1	1.1 ± 0.1	817 ± 64	309 ± 35	12.9 ± 1.7
B1	20.0 ± 2.3	2.2 ± 0.9	118 ± 38	118 ± 9	46.1 ± 0.8
B2	9.9 ± 1.9	1.6 ± 0.5	185 ± 19	154 ± 17	31.5 ± 3.6
B3	9.7 ± 2.0	4.5 ± 1.4	290 ± 86	183 ± 28	32.2 ± 7.8
B4	9.2 ± 0.3	1.7 ± 0.8	221 ± 13	179 ± 10	32.2 ± 1.0
B5	10.5 ± 0.7	2.1 ± 0.1	187 ± 25	135 ± 17	26.3 ± 2.0
B6	20.2 ± 3.3	2.6 ± 0.9	101 ± 21	108 ± 22	43.2 ± 2.7

Note Uncertainties are reported as ± one experimental SD calculated over three independent observations for each chair type, except chair B2 for which only two independent observations are available

Further evidence is provided by Fig. 11, which clearly shows the effect of bottom ignition on HRR for a representative B6 mockup. The heat release rate stabilized to a value of HRR ≈ HRR_{BI} throughout the HRR plateau phase; the end of the HRR plateau phase coincided with the time of bottom ignition of the seat cushion. A similar trend was observed also with the other barriers, even though a moderate temporary increase in heat release rate ($PHRR_1$) was observed during the plateau phase. Ultimately, a large increase in HRR was observed for $t > t_{BI}$ in all tests, thus, it is reasonable to assume that: (a) t_{BI} is a good indicator of the "time to failure" for the barrier tested and (b) bottom ignition is the triggering mechanism that leads to barrier failure. Figure 11 also shows that HRR_{BI} can be used as a good approximation for the HRR at the plateau.

Compared to FPUF pillows, polyester fiber–filled pillows were shown to generate about half the total heat release and produce about five times more char [78]. Regenerated polyols account for about 70% of the total heat released by the FPUF, hence, understanding how and when regenerated polyols become involved in the burning process is extremely important [77].

In Fig. 11, the burning process of the chair mock-up is divided into stage I and stage II, where t_{BI} is the time at which stage I transitions to stage II. During stage I, HRR is mainly supported by gaseous pyrolyzates released through the barrier envelope, which remains intact. At the beginning of stage II ($t = t_{BI}$), liquid products percolating through the barrier envelope (mainly regenerated polyols) ignited and led to a rapid-fire growth. Most of the heat of combustion was released in this phase due to the involvement of regenerated polyols. The heat released during stage II ranged from a minimum average value of 54% THR for chair B1 to a maximum of 87% THR for chair C0.

The barrier failure mechanism described here largely agrees with the observation of so-called "basal melt fire," the failure mechanism previously described in the pioneering work of Ohlemiller and Shields [21]. In the basal melt fire mechanism,

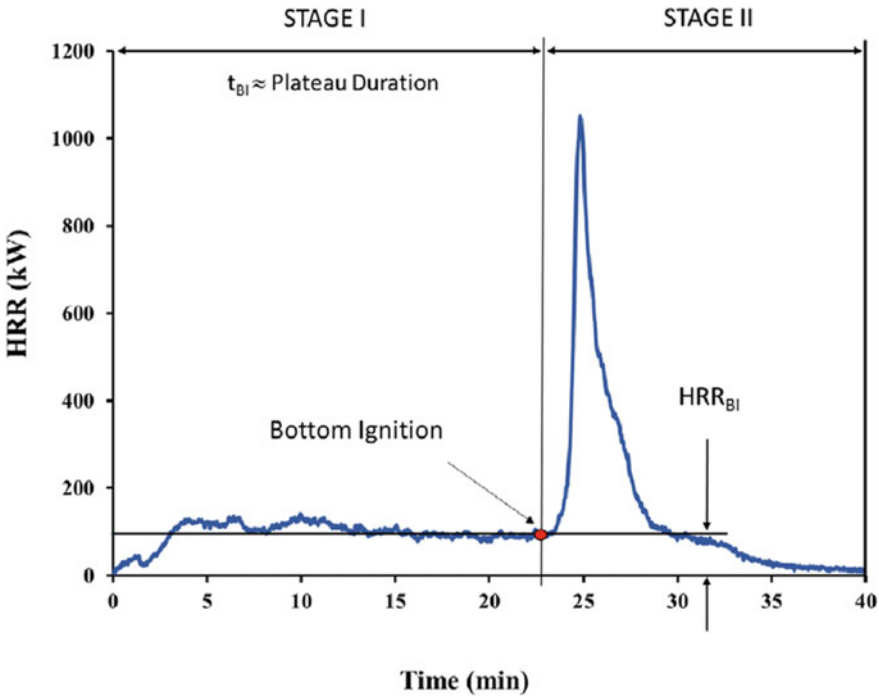

Fig. 11 Effect of bottom ignition on the heat release rate for a representative B6 chair [29]

flames become established on the bottom of a vertically oriented cushion (e.g., seat-back or arm cushion) whose barrier is completely intact. The fuel for the flames was initially the cover fabric but increasingly became the FPUF regenerated polyols as these liquid products were flowing down through the pores in the barrier at the base of the cushion. Based on these considerations, NIST recently developed a bench-scale test (the "Cube Test" mentioned in Sect. 9.2 of this chapter) aiming to predict time to barrier failure at full scale [31, 32].

3.5 Impact of Barriers on Fire Risk

Barriers were found to possibly fully extinguish flaming and prevent a complete combustion of the RUF item when small candle-like ignition sources were used [28]. However, flame extinguishment is not likely with larger ignition sources, like an 18 kW burner; in this scenario, barriers have been found to decrease the burning rate but not necessarily reduce the total heat release [21]. About 10% of RUF fire deaths are due to small flames and about 21% are due to open flames spreading from other items, where the flaming insult to the RUF is likely to be more severe than a candle-like flame [3]. RUF ignition over the seat cushion and alongside the back

cushion led to a shorter time to peak of HRR compared to ignition alongside the arm or under the seat cushion [79].

Based on these considerations, in this study, we selected an 18 kW flame (mimicking the combustion of five sheets of crumpled newsprint) [58] as the ignition source, and the center–top of the seat cushion in proximity of the back cushion as the ignition location. A small bedroom typically requires HRR of about 1000 kW to reach flashover [68]. Flame spread to the surrounding combustibles is unlikely to occur for $t < t_{HF20}$ (i.e., when the heat flux at a distance of 50 cm from the RUF item is below 20 kW/m^2). In the presence of barriers, $t_{HF20} \geq t_{BI}$, and the HRR of the RUF item at $t = t_{BI}$ (HRR_{BI}) is always well below 1000 kW (HRR_{BI} ranges between about 100 and 300 kW). Based on these considerations, it can be concluded that flashover is not likely to occur for $t < t_{BI}$. Similarly, adopting the aforementioned 400 kW criterion for tenability, the conditions in the room will likely remain tenable for $t < t_{BI}$.

In a living room layout where multiple upholstered chairs are placed in close proximity, flame spread to the surrounding combustibles cannot be excluded for $t < t_{HF20}$ because the heat flux on the combustible can reach the critical value of 20 kW/m^2 for nonpiloted ignition. Also, piloted ignition (which requires a critical heat flux as low as 10 kW/m^2) [74] becomes likely for distances below 50 cm due to flickering flames or hot objects (projected by the RUF fire), which can act as an ignition source. Nevertheless, the use of barriers is expected to significantly reduce the fire hazard also in this scenario, especially if the second item ignited is also an RUF item protected by a barrier; in fact, in this case the second item ignited will also show a HRR plateau and consequent delay in peak of HRR. A 15-min delay time to flashover and 12 min increase in estimated available safe egress time (ASET) were achieved by using barrier B6 to protect a sofa in a fully furnished living room selected as case study; this reduction in fire growth would likely allow first responders to intervene and prevent flashover [77]. Due to the severity of the test conditions in the case study, it is not unrealistic to expect that first responders would be able to intervene before flashover in a large fraction of room fire scenarios where an effective barrier like B6 is adopted.

The dominant mechanisms by which the barriers mitigated the fire hazard of the chair mock-ups were: (a) delay in fire growth (the longer the time to bottom ignition, the longer the time available for egress before untenable conditions are reached and for first responders to arrive and attack the fire), and (b) a reduction in $PHRR_2$ (the lower the PHRR, the lower the likelihood of flashover and flame spread occurrence) [67, 80]. B1 and B6 were the best performing barriers in terms of t_{BI} and $PHRR_2$ (B6 being the best due to the absence of $PHRR_1$ and lower initial HRR). Interestingly, both B1 and B6 contain hybrid yarns made of regenerated cellulose and polysilicic acid, which are inherently fire resistant [36]. Polysilicic acid is an inorganic material that decomposes endothermically to release water and dilute combustible products of decomposition [36, 39]. In addition, the incorporation of molecular chains of silicic acids into the hybrid yarn is expected to improve barrier performance by increasing the cellulose char yield [39].

A delay of t_{BI} from about 2 min (control chair) to about 20 min (B1 and B6 chairs) can be contextualized by analyzing the objective (target) fire service response times. A properly placed smoke alarm can be activated within about 40 s even with RUF items using the best performing barrier B6 [30]. Based on NFPA 1710 [81] and NFPA 1720 [82], first responders are expected to intervene within about 12 min in urban areas, 13 min in suburban areas, and 17 min in rural areas [30]. An RUF with similar fire growth as for the chair mock-ups without barrier (i.e., $PHRR_2$ above 2500 kW and $t_{P2} \approx 3$ min) would most likely lead to flashover before responders intervention even in urban areas [67], whereas, an RUF with a reduced fire growth as for the chair mock-ups with B6 ($t_{BI} \approx 20$ min) would most likely allow responders to intervene before flashover even in rural areas because, as previously discussed, flashover is not likely to occur for $t < t_{BI}$.

4 Fire Barriers in Furnished Compartments

4.1 Test Setup and Procedure

The goal of Sect. 9.4 is to determine if the failure mechanism of barrier fabrics previously observed in the chair mock-up experiment (Sect. 9.3) also applies to commercial RUF in furnished compartments. B6 has been used in a commercial couch for full-scale compartment tests in a realistic fire scenario. The objectives of this section include: (1) quantifying the effect of barrier fabrics on the fire hazard (e.g., tenability conditions, heat release rate, time to flashover and smoke generation) of RUF ignited by a flaming-ignition source in a realistic living room scenario, (2) show that barrier fabrics, which can remarkably reduce the fire hazard without using chemically active fire retardants, not only exist but are commercially available, and (3) d etermine if the failure mechanism of barrier fabrics previously observed in the chair mock-up experiment also applies to commercial RUF in a realistic scenario.

RUF compositions used in this study can be found in Zammarano et al. [30]. Three fire tests, one per couch type, were conducted. In Test 1, the couch with the polyester covering was used. In Test 2, the cotton blend covering was used in combination with the barrier fabric. In Test 3, the same cotton blend covering of Test 2 was used without barrier fabric. The schematic drawing of the couch and additional items with dimensions, composition, mass, and quantity can be found in Zammarano et al. [30]. A picture of the test setup in shown in Fig. 12.

The instrumentation used in these experiments to measure HRR, incident heat flux, gas temperature, and description of air-cooled cameras under the loveseat and chaise sections of the couch are summarized in detail in Zammarano et al. [30].

Fig. 12 Picture of furnished compartment test setup under the 10 MW hood at the National Fire Research Laboratory [30]

4.2 Observations and Heat Release Rate

For all tests, the smoke alarm triggered within the first minute after fire ignition (42 s in Test 1, 47 s in Test 2 and 45 s in Test 3) presumably due to the rapid burning of the throw pillow. The burning behavior varied significantly between samples without a barrier fabric (Test 1 and Test 3) and the sample with a barrier fabric (Test 2). Figure 13 compares snapshots of the three tests at 2 min, 4 min, 6 min and 8 min from ignition. At 2 min, a similar smoke layer, flame spread and flame size were observed in all tests. In Test 1 and Test 3, after 2 min the flame spread and fire intensity increased continuously until flashover conditions were reached. In Test 2, after 2 min the flame spread decreased; 4 min after ignition, the smoke layer dissipated and did not reappear until approximately 10 min later in the test. The photographs in Fig. 13 qualitatively demonstrates the efficacy of the barrier fabric to reduce flame spread over the couch.

Figure 14 shows the heat release rates for Test 1, Test 2, Test 3, and Throw Pillow 1 during the first 500 s after ignition. A lower heat release rate was expected for Test 2 as compared to Test 3 due to the inclusion of the barrier fabric. The lower heat release rate for Test 1 as compared to Test 3, however, is surprising because cotton blend cover fabrics are typically expected to be less flammable than polyester cover fabrics even though the behavior of fabric blends are often unpredictable [21].

The heat release rate curves from ignition to extinguishment for Test 1, Test 2 and Test 3 are shown in Fig. 15. The values of peak heat release rate (PHRR), time

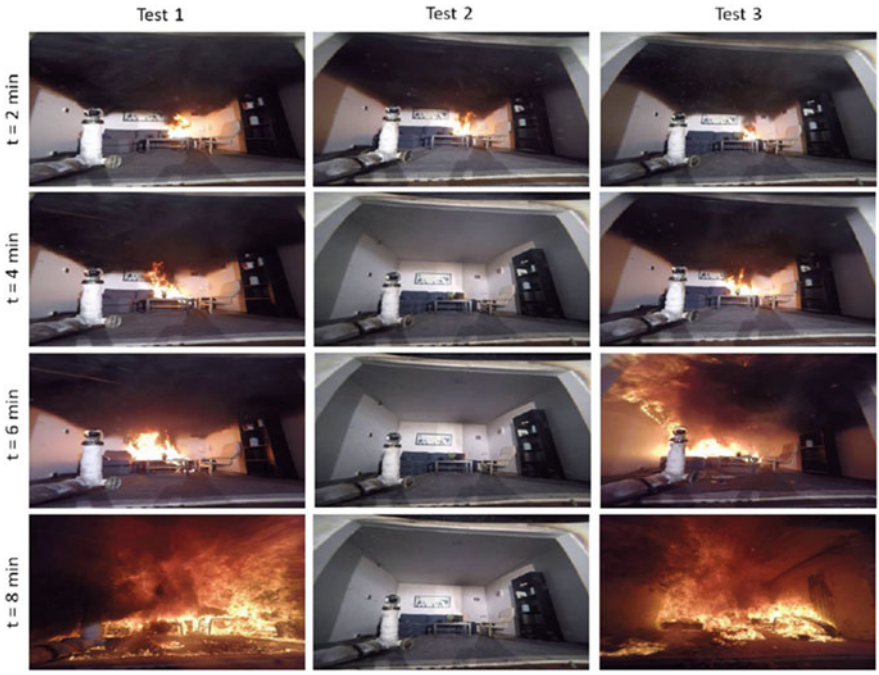

Fig. 13 Photographs of the compartments at 2 min, 4 min, 6 min and 8 min after ignition. These photographs qualitatively demonstrate the efficacy of the barrier fabric. At t = 2 min, a similar smoke layer, flame spread and flame size were observed in all tests. For t > 2 min, the flame spread and fire intensity increased continuously in Test 1 and Test 3, until flashover conditions were reached. In Test 2, the flame spread decreased; at t = 4, the smoke layer dissipated and did not reappear until approximately 10 min later [30]

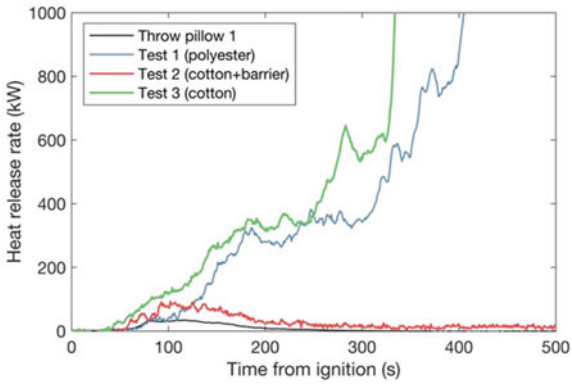

Fig. 14 Heat release rate curves measured for Test 1 to Test 3 and for the Throw pillow 1 during the first 500 s after ignition [30]

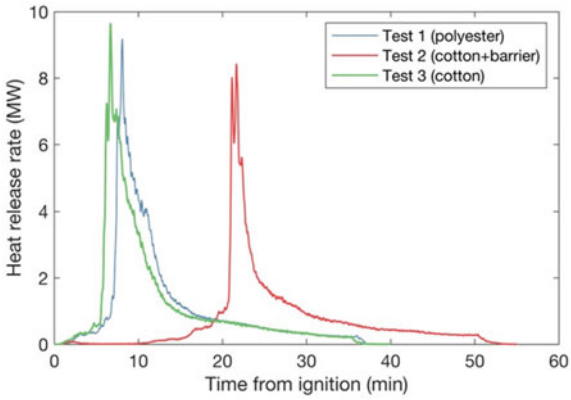

Fig. 15 Heat release rate curves for Test 1, Test 2, and Test 3 [30]

Table 5 Values of time to peak heat release rate t_{PHRR}, peak heat release rate (PHRR) and total heat release rate (THR) measured in Test 1, Test 2, and Test 3 [30]

	t_{PHRR} (min)	PHRR (kW)	THR (MJ)
Test 1	9.1 ± 0.2	9180 ± 550	2550 ± 160
Test 2	21.7 ± 0.2	8420 ± 500	2250 ± 140
Test 3	6.7 ± 0.2	9640 ± 580	2640 ± 160

to peak heat release rate (t_{PHRR}), and total heat release (THR) are summarized in Table 5. All tests were extinguished with water about (25 to 30) min after PHRR.

t_{PHRR} showed substantial variations. The t_{PHRR} was (6.72 ± 0.17) min for Test 3, (9.12 ± 0.17) min for Test 1, and (21.68 ± 0.17) min for Test 2. Compared to Test 3, the use of the barrier fabric with the same cover fabric in Test 2 offered a 300% increase in t_{PHRR} (i.e., it took approximately 3 times longer for the PHRR to be observed when a barrier fabric was used). This increase in t_{PHRR} was associated with the formation of a quasi-steady state burning with a minimum heat release rate plateau value of about 15 kW at $t \approx 8$ min in the early burning stage of Test 2 when the combustion of the throw pillow was complete. The THR in Test 2 decreased by about 15% compared to Test 3 due to the addition of the barrier fabric to the cotton blend cover fabric.

4.3 Flashover

Flashover is the last phase in fire growth that leads to a fully-developed compartment fire. Flashover occurs when the room is hot enough (or heat transfer from the upper smoke layer is large enough) that all combustible solids in the room begin pyrolyzing and producing gaseous volatiles, despite the presence or absence of direct flame impingement. Ignition of these gaseous pyrolyzates yields an abrupt increase in heat release rate [83]. In this study, it is assumed that flashover conditions in the

compartment were reached when the magazines and the single upholstered chair ignited almost simultaneously. The time to flashover and the time to smoke alarm triggering for Test 1 to Test 3 are reported in Table 6.

The smoke alarm triggering times were similar for all tests. The time to flashover increased by less than 1 min when the cotton blend cover fabric (Test 3) was replaced by the polyester cover fabric (Test 1). Thus, the effect of the cover fabric was statistically significant, but small. In comparison, the influence of the barrier fabric on the time to flashover was large. The presence of the barrier fabric delayed the time to flashover by about 15 min in Test 2 (cotton blend cover fabric and barrier fabric) compared to Test 3 (cotton blend cover fabric only).

The rapid fire growth observed in Test 1 and Test 3 may present a significant hazard to life and property before first responders can arrive. Thus, a 15 min delay of flashover observed in Test 2 can drastically reduce this hazard. This can be contextualized by analyzing the objective (target) fire service response times in NFPA 1720 [82]. The target response time is 9 min in urban areas (for at least 90% of the responses), 10 min in suburban areas (for at least 80% of the responses), and 14 min in rural areas (for at least 80% of the responses). Response time begins upon completion of the dispatch notification to the fire department and ends at the time a prescribed number of staff members start mitigation measures at the fire scene. After ignition, assuming an average smoke alarm triggering time of 45 s, an alarm answer time of 15 s to 40 s and an alarm processing time of 64 s to 106 s (see NFPA 1710 for response objectives [82]), the response time will start about 2 min to 3 min after ignition. Thus, considering the target response time, the first responders are expected to intervene within 12 min in urban areas, 13 min in suburban areas and 17 min in rural areas. A graphic representation of time to flashover for Test 1, Test 2, and Test 3 versus response time is shown in detail in Zammarano et al. [30].

If these experiments are representative of available couches, the data suggests that first responders may not be able to intervene before flashover when a couch without barrier fabric is involved in the types of compartment fires represented by Test 1 and Test 3, even in urban areas. However, under the same conditions, first responders would likely be able to intervene and prevent flashover when a barrier fabric is adopted in the couch (Test 2) in urban, suburban, and rural areas. Flashover prevention is critical because it can prevent fire spread to adjacent rooms and buildings, which is where the majority of fire deaths occur in RUF fires [2].

Figure 16 shows video frames at flashover for Test 1, Test 2, and Test 3 captured by the water-cooled camera, the 360° camera, and the air-cooled camera under the chaise section of the couch. The water-cooled camera (top row in Fig. 16 shows that

Table 6 Time to smoke alarm triggering and flashover in Test 1, Test 2, and Test 3 [30]

	Time to smoke alarm triggering (s)	Time to flashover (min)
Test 1	42 ± 2	7.0 ± 0.2
Test 2	47 ± 2	21.0 ± 0.2
Test 3	45 ± 2	6.0 ± 0.2

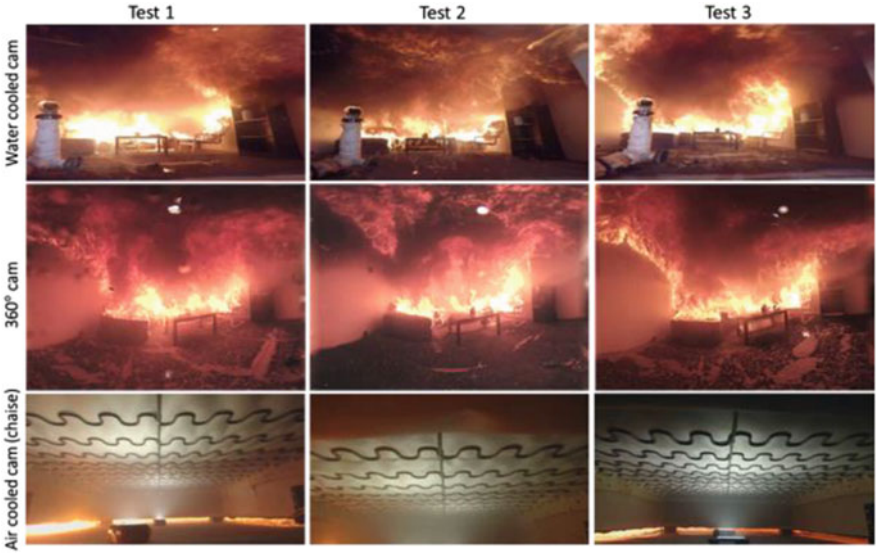

Fig. 16 Video frames at the time of flashover for Test 1 (left column), Test 2 (center column), and Test 3 (right column) captured by the water-cooled camera (top row), 360° camera (center row), and air-cooled camera under the chaise section of the couch (bottom row) [30]

by the time flashover occurred, flames appeared to cover the entire couch except the front vertical surface of the chaise section. The 360° camera (middle row in Fig. 16) confirms this for Test 1 and Test 3, however, for Test 2, it also shows that flame spread over the top surface of the chaise section was not complete, i.e., flaming was not present over the extremity of the top seat cushion which was opposite to the back cushion. The air-cooled cameras under the chaise section (bottom row in Fig. 16) show that there was no flaming underneath the chaise section at flashover for all tests.

The presence of flaming underneath the RUF item is important because it increases: (1) the incident heat flux on the couch padding material where most of the fuel, i.e., FPUF, is located and thus, (2) the rate of FPUF pyrolysis, (3) the rate at which combustible volatiles are released, and (4) the rate at which liquid product of FPUF decomposition (i.e., regenerated polyols [35]) are generated. All these phenomena promote an increase in heat release rate. Flaming under the loveseat section is initially due to the ignition of the polyester wadding and cover fabric on the bottom of the seat cushion and, afterwards, the ignition of regenerated polyols. The flaming ignition of regenerated polyol underneath the RUF item, referred to as "bottom ignition" as previously discussed throughout this chapter, is particularly important because about 70% of the FPUF heat released is due to regenerated polyol combustion [77]. Figure 17 shows video frames captured by the air-cooled cameras under the loveseat section at various times during Test 1 (top row), Test 2 (center row), and Test 3 (bottom row). In all cases, no obvious degradation was observed at $t = 6$ min (compare column 1 to column 2).

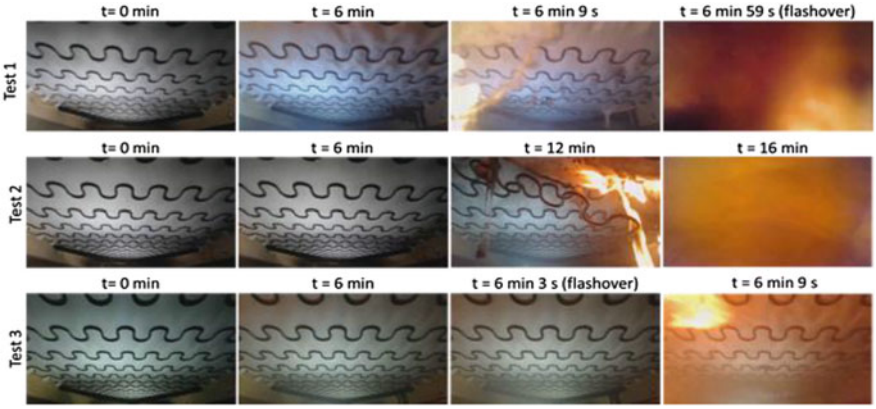

Fig. 17 Video frames captured by the air-cooled cameras under the loveseat section at various times during Test 1 (top row), Test 2 (center row), and Test 3 (bottom row) [30]

In Test 1, flaming became visible at about 6 min 9 s and was caused by the formation of a pool fire underneath the couch. The pool fire was generated by flaming liquids produced on the top of the seat cushion that flowed from the front of the loveseat section to the floor. In this test, flashover occurred about 50 s after flaming appeared under the loveseat section. At this time a significant flame spread underneath the loveseat section was observed in Test 1 (see video frame in the top row on the far right). Thus, bottom ignition briefly contributed to flashover conditions in Test 1, but the pool fire was mainly fed by the top of the seat cushion. In Test 3, flames appeared in the same location and by the same mechanism observed for Test 1 but a few seconds after flashover. Thus, flashover conditions could be reached in Test 3 without any contribution from bottom ignition. In Test 2, flames appeared at about 12 min in the back- right corner of the sofa, i.e., northwest corner of the couch. At this early stage, flaming under the loveseat section was likely supported by burning of the polyester wadding and the cover fabric but not by FPUF, which was protected by the barrier fabric. Flames continued to spread under the loveseat and by $t = 16$ min the bottom right of the loveseat was engulfed in flames.

To better describe the phenomena that led to flashover in Test 2, Fig. 18 shows four video frames captured by the 360° camera 6 min, 8 min, 10.2 min, and 18 min after ignition. At $t = 6$ min, the combustion of the throw pillow was complete and the heat release rate was below 15 kW. Flames were localized to the right side of the couch on the top of the seat cushion and front of the back cushion. At $t = 8$ min the heat release rate was still below 15 kW but the flames propagated to the back of the couch where the polyester wadding fabric, and wood frame were not protected by the barrier fabric and an increase in flame size was observed near the back right corner. Noticeably, only the padding material, i.e., FPUF and polyester fiberfill, were protected and covered by the barrier fabric. At $t = 10.2$ min, the flame spread further over the back of the couch and the HRR increased to about 30 kW. It was evident that the combustion of the back of the couch sustained flaming and promoted an

Fig. 18 Video frames captured during Test 2 at t = 6 min, 8 min, 10.2 min, and 18 min [30]

increase in HRR. These observations indicate that the addition of barrier fabric over the back of the couch could have further improved the fire performance of the couch. Shortly after at $t = 12$ min, flames had spread to the bottom of the loveseat. At $t = 18$ min, an obvious pool fire formed underneath the loveseat section. This is a clear indication that, by this time in the test, bottom ignition occurred, and the regenerated polyols were involved in the burning process. An abrupt increase in HRR observed at approximately $t = 17$ min could be attributed to bottom ignition. Bottom ignition preceded flashover in Test 2, which occurred at about $t = 20.9$ min, by roughly 3 min. This finding agrees with previous work where the PHRR occurred about 2 min to 4 min after bottom ignition [29] discussed in Sect. 9.3.

4.4 Heat Flux and Tenability Conditions

Figure 19 shows the heat fluxes measured on the couch near the ignition location (PTC4). In Test 1 and Test 3, the heat flux reached about 75 kW/m^2 after about 4 min. These data suggest that values of incident heat flux over 50 kW/m^2 are advisable for a robust evaluation of the fire performance of barrier fabric at bench scale. Values of incident heat flux of 75 kW/m^2 were adopted in the Cube Test for ranking the performance of barrier fabrics [31] described in Sect. 9.2. In Test 3, the heat flux peaks at about 10 kW/m^2 at about 2 min when the throw pillow is still burning, and then drops to below 5 kW/m^2 until bottom ignition. After flashover the heat flux reached peak values above 150 kW/m^2 in all three tests. Noticeably, the highest peak value was achieved in Test 2 (about 200 kW/m^2) despite the presence of the barrier fabric, possibly due to the strong and prolonged flame heat feedback between the pool fire and the unburned portions of the couch. The heat fluxes along the wall

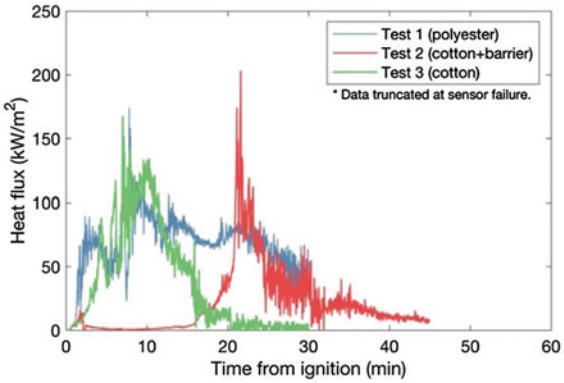

Fig. 19 Heat flux measured on top of the couch near the ignition location (PTC4) for Test 1, Test 2, and Test 3 [30]

reached the highest values at PTC3 close to the ceiling; the peak value of heat flux was about 175 kW/m^2 in Test 1 and Test 3 and about 150 kW/m^2 for Test 2.

During and immediately after a fire, conditions may become untenable such that the occupants are incapacitated and cannot escape by themselves, in which case they are likely to die unless rescued. The leading cause of incapacitation and death during and immediately after fires is exposure to asphyxiant gases: carbon monoxide (CO), hydrogen cyanide (HCN), and carbon dioxide (CO_2), with some additional effects from low-oxygen hypoxia and inhaled irritants [73]. The effect of fire effluents on incapacitation can be estimated using the Fractional Effective Dose [84]. In upholstery furniture flammability without chemical fire retardants, carbon monoxide is the main hazard, although the contribution of hydrogen cyanide is also significant [85, 86]. The CO concentration at which there is danger of incapacitation after approximately 5 min exposure in a person engaged in light activity is about 6000 ppm to 8000 ppm [73]. These values are never reached in these tests (see Fig. 20) due to the high ventilation factor of 0.14 m$^{1/2}$ but could be easily achieved in more realistic room scenarios [85].

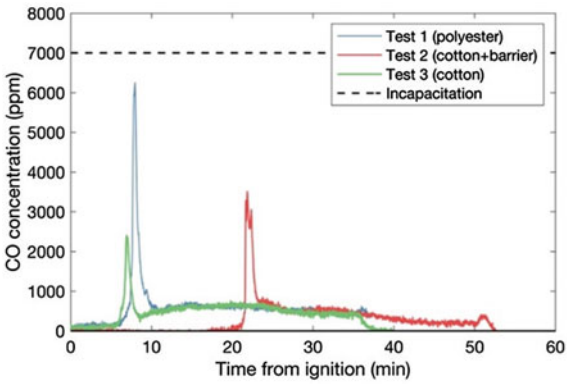

Fig. 20 CO concentration measured for Test 1, Test 2, and Test 3 and CO incapacitation level after approximately 5 min exposure [30]

Table 7 Time at which an upper layer temperature of 200 °C at $T_{ceiling}$ ($t_{200\,°C}$) and flux of 2.5 kW/m^2 at PTC2 ($t_{2.5\,kw/m^2}$) were met and calculated Available Safe Egress Time (ASET) [30]

	$t_{200\,°C}$ (min)	$t_{2.5\,kW/m^2}$ (min)	ASET (min)
Test 1	3.92	3.33	2.63
Test 2	16.03	16.56	15.25
Test 3	3.05	3.05	2.30

Alternate tenability criteria include: a maximum upper layer gas temperature of 200 °C and an exposure to radiant heat fluxes above 2.5 kW/m^2 [73]. For each test, Table 7 shows the times at which: (1) a temperature of 200 °C at $T_{ceiling}$ was reached ($t_{200\,°C}$), and; (2) a heat flux of 2.5 kW/m^2 was reached at PTC2 ($t_{2.5\,kW/m^2}$). The smaller between $t_{200\,°C}$ and $t_{2.5\,kW/m^2}$ is used to estimate the time at which untenable conditions were reached. These data indicate that untenable conditions were reached before flashover and, thus, heat exposure rather than gas toxicity seems to be the main hazard in this scenario.

Table 7 also shows the Available Safe Egress Time (ASET) in the enclosure fire calculated as the time between smoke alarm triggering (see Table 7) and the onset of untenable conditions [87]. Available Safe Egress Time values below 3 min for both Test 1 and Test 3 indicated an extremely high fire hazard. The adoption of a barrier fabric in Test 2 allowed a significant increase in the ASET value from about 3 min to about 15 min which would drastically increase the likelihood of survival for an occupant.

5 Conclusions

In the fire barriers in reduced scale testing section, a cone-calorimetry-based bench-scale test (the "Cube" test) was developed to capture mass and heat transfer phenomena at the top and bottom of a specimen. The Cube test was designed to mimic the burning process of cored composites where the flammable core material acts as the main fuel load and superficial layers may act as fire barriers. Results showed the mass transfer of flammable liquid products underneath the specimen (due to percolation of liquid products through the bottom fire barrier, which can lead to dripping and pool fire formation in upholstered furniture) captured in the Cube test.

Appropriate test conditions were determined in which the specimen decomposition pathway in the Cube test was representative of full-scale upholstered furniture fires. Specifically, an external heat flux of 75 kW/m^2 was required to "liquify" the foam to produce liquid pyrolyzates without significant char formation, thus allowing for measurement of the time required for the appearance of liquid pyrolyzates under the specimen as wetting of the fire barrier (time to wetting). Based on the values of time to wetting (t_w), the best performing fire barrier was B3 ($t_w = 258$ s $\pm$ 7 s), followed by B1($t_w = 235$ s $\pm$ 17 s), B6 ($t_w = 222$ s $\pm$ 2 s), B5 ($t_w = 164$ s $\pm$ 4 s),

B2 ($t_w = 153$ s $\pm$ 2 s), and B4 ($t_w = 143$ s $\pm$ 2 s). As expected, the control sample without fire barrier had the worst performance ($t_w = 90$ s $\pm$ 3 s).

In a fire scenario it was proposed that: (a) the time to wetting may be used to predict the time to "fire barrier failure" in full-scale tests (time at which a rapid increase in heat release rate is expected due to the percolation and ignition of flammable liquids beneath the RUF item), and; (b) the average heat release rate in the Cube test prior to t_w may be used to predict the average heat release rate before fire barrier failure in upholstered furniture items. An analytical approach to connect these bench-scale measurements to quantitative measurements of burning behavior in full-scale tests has been introduced in Zammarano et al. [31] and was assessed in another paper by Zammarano [32]. Even when the assumptions on the fire scenario are not perfectly fulfilled, the Cube test might still be adopted to rank the relative performance of fire barriers when used in full-scale experiments as it captures the mass and heat transfer effects of the fire barrier in a well-defined, realistic fire scenario.

In the fire barriers in full-scale testing chair mock-ups section, a twofold objective were explored: (a) reveal to what extent barriers, which do not contain chemical FR additives (passive barriers), can decrease the fire risk of upholstered chair mock-ups when exposed to a strong (18 kW) ignition source, and (b) investigate the mechanism leading to the failure of barriers. Six commercially available barriers (B1 to B6) contained inherently FR fibers, but no additional chemical FR according to the manufacturers. This was confirmed by independent chemical analyses, whose findings showed that there was an insufficient presence of common FRs to significantly affect the performance of the barriers.

This series of fire tests demonstrated that none of the barriers were able to prevent ignition of the padding material, and the cushions in all chairs eventually burned to completion with marginal differences in total heat release. However, all barriers significantly decreased the fire growth of the chair mock-ups by generating an initial plateau with reduced heat release rate. The second, dominant peak heat release rate was remarkably delayed from about 3 min for the control chair to as much as 22 min for the best performing barriers; similarly, the peak heat release rate was reduced from about 2.6 MW to approximately 1 MW. The heat release rate of a mock-up without a barrier was enough to lead to flashover in most rooms in less than 3 min, whereas, the use of an effective barrier sufficiently delayed the fire growth to likely allow occupants to escape and enable first responders to intervene before flashover and, thus, prevent many fire deaths. Additionally, barriers mitigated the fire hazard by increasing the time available for egress and by decreasing the likelihood of flame spread. Barrier B6 appeared to be the best performing barrier based on its low heat release at its HRR plateau (<200 kW), its low peak heat release rate ($\approx$1 MW), and its prolonged time to peak ($\approx$23 min).

A common failure mechanism was identified for all barriers. This was not a mechanical or thermal failure of the barrier; instead, it was associated with the so-called "bottom ignition," that is, the ignition of liquid pyrolizates which percolated through the barrier underneath the seat cushion. Based on these findings, a bench-scale test ("Cube test") aiming to predict time-to-barrier failure at full scale was being developed. The understanding of the barrier failure mechanism is also expected to

assist manufacturers and scientists toward the development of barriers and upholstery products with improved fire performance.

In the fire barriers in full scale testing: furnished compartments section, a series of three full-scale compartment fire experiments helped characterize the potential fire hazard of residential upholstered furniture (RUF) and the potential ability of a barrier fabric to decrease such hazard. A representative living room was constructed and furnished identically except for three different couches that were the same except for the following: Test 1—couch with polyester cover fabric in Test 1; Test 2—couch with a cotton blend cover fabric and a barrier fabric (made of intrinsically fire-resistant fibers without any additional fire retardant; and Test 3—couch with only a cotton blend cover fabric (same cover fabric as Test 2).

A throw pillow on the right arm of the couch ignited using a 3 cm propane diffusion flame acted as an ignition source for each of the couches. From this set of experiments, the results demonstrated the use of a fire barrier without chemically active flame retardants can remarkably delay the growth of RUF fires. The two couches without a barrier fabric, which were compliant with TB-117–2013, posed a severe fire hazard with rapid fire growth leading to flashover within approximately 6 min of ignition. The addition of the barrier fabric delayed flashover by about 15 min from about 6 min to 21 min, and increased the estimated Available Safe Egress Time (ASET) from less than 3 min to over 15 min.

Considering target fire service response times, this delay is important because it allows first responders additional time to intervene before flashover (alarming time plus response time is typically 12 min to 17 min depending on whether the location is urban or rural) and potentially prevent flashover occurrence. Flashover prevention is critical because it can stop fire spread to adjacent rooms and building; where most fire losses occur. The barrier fabric in these experiments covered all padding material but not the back of the couch, where flaming rapidly spread over the wadding and cover fabric once ignited. Thus, a further improvement in fire performance could be expected if the back of the couch was also protected by additional barrier fabric.

The presence of the barrier fabric also affected the mechanism by which flashover conditions were reached and the role of pool fire formation. Without barrier fabric, flashover conditions could occur before a regenerated polyol pool formed on the floor with little to no flaming on the bottom of the couch. With the barrier fabric, flashover occurred several minutes after the appearance of flaming underneath the couch and the formation of a pool fire; pool fire increased the pyrolysis rate of the residual padding material and, in turn, caused an additional increase in heat release rate that led to flashover.

In summary, the set of data suggest that: (a) despite compliance with cigarette ignition tests, residential upholstered furniture may still pose a considerable fire hazard due to rapid fire growth and flame spread in presence of a flaming ignition source; (b) technologies promoting fire safety and health/environment safety for residential upholstered furniture are not mutually exclusive as these tests demonstrate that non-toxic technologies, which can meet both requirements, not only exist but are commercially available; (c) the presence of a barrier fabric resulted in a 15 min delay in time to flashover and 12 min increase in estimated ASET drastically decreased

the fire hazard; (d) the mechanisms that lead to failure of the barrier fabric and consequent flashover in the compartment appear to be triggered by the ignition of liquid pyrolyzates percolating through the bottom barrier fabric in the residential upholstered furniture item.

In this chapter of new fire protection materials, an overall review of fire barriers was studied as a potential solution to reduce residential upholstered furniture (RUF) flammability. The fire barriers studied in this chapter did not contain chemical fire-retardant additives (passive barriers) and were shown to decrease the fire risk of RUF when exposed to a strong ignition source. Fire barriers were used in a reduced scale testing method (cube test), large scale testing method (chair mock-ups), and real-life scenario testing method (RUF in furnished compartments). In each testing method, the fire barriers were placed between padding materials and was shown to reduce fire growth rate after flaming ignition by limiting heat transfer to a flammable substrate and controlling the rate and location at which volatiles are released and able to burn. Additionally, barriers mitigated the fire hazard by increasing the time available for egress and by decreasing the likelihood of flame spread which provides additional time for firefighters to prevent flashover. The heat and mass transfer effects were physically based thus no chemical fire retardants were needed. A common failure mechanism was identified for all barriers. It was not a mechanical or thermal failure of the barrier; instead, it was associated with the ignition of liquid products which percolated through the barriers. The use of barriers is expected to significantly reduce the fire hazard, especially if the second item ignited is also an RUF item protected by a barrier. The data from the HRR curves in this chapter are useful for modeling second item ignitions to create more realistic fire cases to generate training data to develop more robust machine learning models. The understanding of the barrier failure mechanism is expected to assist manufacturers and scientists toward smart firefighting and the development of barriers and upholstery products with improved fire performance.

Acknowledgements The author gratefully acknowledges Mauro Zammarano, Leader, "Fire Barriers for Low Heat Release Rate Products" Project at the National Institute of Standards and Technology (NIST) for his mentorship and guidance throughout the various projects cited in this chapter. Also, the team at the NIST National Fire Research Laboratory—Matthew Bundy, Matthew Hoehler, Anthony Hamins, Marco Fernandez, Laurean DeLauter, Philip Deardorff, Anthony Chakalis, Michael Selepak, Artur Chernovsky, and Andrew Mundy—for their assistance in test setup, execution, and expertise made various experiments cited in this chapter possible. Members of the NIST Flammability Reduction Group—Ickchan Kim, John R. Shields, Isaac Leventon, Shonali Nazare, Rick Davis, William Pitts, and Richard Gann for their valuable contributions. Special thanks are given to the NIST Fire Department for their support for each burn conducted in NFRL.

References

1. M. Ahrens, *Home Structure Fires* (National Fire Protection Association, 2019)
2. M. Ahrens, *Home Fires that Began with Upholstered Furniture* (National Fire Protection Association Research, 2017).
3. J.R. Hall, Estimating fires when a product is the primary fuel but not the first fuel, with an application to upholstered furniture. Fire Technol. **51**(2), 381–391 (2015)
4. R.G. Gann, The challenge of realizing low flammability home furnishings. Interflam, in *Interscience Communications* (CD Version, London, England, 2013)
5. Anonymous: Requirements, Test procedure and apparatus for testing the smolder resistance of materials used in upholstered furniture, in *Bureau of Electronic & Appliance Repair Home Furnishing & Thermal Insulation, Technical Bulletin*, vol. 117 (Sacramento, CA, 2013)
6. Anonymous: filling/padding component test method—barrier test method—fabric classification test method. Upholstered Furniture Action Council (UFAC) (1990)
7. A. International, *E1353–16 Standard Test Methods for Cigarette Ignition Resistance of Components of Upholstered Furniture* (ASTM International, West Conshohocken, PA, 2016)
8. Agency NFPA: NFPA 260—Standard Methods of Tests and Classification System for Cigarette Ignition Resistance of Components of Upholstered Furniture (2013)
9. Anonymous: PART 1640—Standard for the Flammability of Upholstered Furniture, Federal Register/Vol. 86, No. 67/in 16 CFR Part 1640 ed Commission CPS (2021)
10. D. Clark, *What is TB117–2013?* (Home Furnishings Association, 2015)
11. I. Watanabe, S.I. Sakai, Environmental release and behavior of brominated flame retardants. Environ. Int. **29**, 665–682 (2003)
12. S.D. Shaw, M.L. Berger, D. Brenner, K. Kannan, N. Lohmann, O. Papke, Bioaccumulation of polybrominated diphenyl ethers and hexabromocyclododecane in the northwest Atlantic marine food web. Sci. Total Environ. **407**, 3323–3329 (2009)
13. S. Mizouchi, M. Ichiba, H. Takigami et al., Exposure assessment of organophosphorus and organobromine flame retardants via indoor dust from elementary schools and domestic houses. Chemosphere **123**, 17–25 (2015)
14. V. Babrauskas, A. Blum, R. Daley, L. Birnbaum, Flame retardants in furniture foam: benefits and risks, in *Paper presented at: Fire Safety Science-Proceedings of the Tenth International Symposium* (2011), pp. 265–287
15. M. Babich, C. Bevington, X. Chen, et al., Project plan: organohalogen flame retardant chemicals assessment. Consum. Prod. Saf. Comm. (2020)
16. An Act to Protect Firefighters by Establishing a Prohibition on the Sale and Distribution of New Upholstered Furniture Containing Certain Flame-Retardant Chemicals. 128th Maine Legislature House of Representatives 182 (2017)
17. Consumer Products: Flame Retardant Materials. State of California Office of Legislative Counsel Bloom 2998 (2018)
18. CPSC-2015–0022 CDN: Guidance document on hazardous additive, non-polymeric organohalogen flame retardants in certain consumer products, in *Commission CPS*, ed., vol. 82: Federal Register (2017)
19. C. Papaspyrides, P. Kiliaris, *Polymer Green Flame Retardants* (Elsevier, Amsterdam, Netherlands, 2014)
20. S. Nazare, W. Pitts, S. Flynn, J.R. Shields, R.D. Davis, Evaluating fire blocking performance of barrier fabrics. Fire Mater. **38**, 695–716 (2014)
21. T.J. Ohlemiller, J.R. Shields, Behavior of mock-ups in the California technical bulletin 133 test protocol: fabric and barrier effects. NIST Interagency/Internal Report (NISTIR) 5653 (1995)
22. W. Pitts, M. Werrel, M. Fernandez, A.M. Long, Assessing the Predictive Capability for Real-Scale Residential Upholstered Furniture Mock-Up Fires using Cone Calorimeter Measurements. Part 1: Real-Scale Experiments (Eisenberg EA, Runyon CD, 2020)
23. T. Fabian, Upholstered furniture flammability, in *Underwriter Laboratories* (2013)
24. W.D. Woolley, S.A. Ames, A.I. Pitt, K. Buckland, The ignition and burning characteristics of fabric covered foams. Build. Res. Establ. (1978)

25. K. Storesund, A. Steen-Hansen, A. Bergstrand, Fire safe upholstered furniture: alternative strategies to the use of chemical flame retardants. SP Fire Res. (2015)
26. A. Lock, *Memoranda on Full-Scale Upholstered Furniture Testing, 2014–2015. U.S. Consumer Product Safety Commission* (2016)
27. A. Lock, *Memoranda on Full-Scale Upholstered Furniture Testing, 2016. U.S. Consumer Product Safety Commission* (2017)
28. M. Black, A. Davis, D. Harris, P. Barry, R. Cohen, et al., *A Study of Chemical Exposure Risk and Flammability of Upholstered Furniture and Consumer Electronics. Underwriter Laboratories* (2019)
29. A.L. Thompson, I. Kim, A. Hamins, M. Bundy, M. Zammarano, Performance and failure mechanism of fire barriers in full-scale chair mock-ups. Fire Mater. **46**(1), 329–346 (2021)
30. M. Zammarano, M.S. Hoehler, J.R. Shields, A.L. Thompson, I. Kim, I. Leventon, M. Bundy, *NIST Technical Note 2129. Full-Scale Experiments to Demonstrate Flammability Risk of Residential Upholstered Furniture and Mitigation Using Barrier Fabric. NIST Technical Note* (2021)
31. M. Zammarano, J.R. Shields, I. Leventon, I. Kim, S. Nazare, A. Thompson, R.D. Davis, A. Chernovsky, M. Bundy, Reduced-scale test to assess the effect of fire barriers on the flaming combustion of cored composites: an upholstery-material case study. Fire Mater. **45**(1), 114–126 (2021)
32. M. Zammarano, *Fire Performance of Upholstery Materials: Correlation between Cube Test and Full-Scale Chair Mock-Ups. NIST Technical Note*, vol. 219 (2021)
33. S. Nurbakhsh, J. Mccormack, A review of the technical bulletin 129 full scale test method for flammability of mattresses for public occupancies. J. Fire Sci. **16**(2), 105–124 (1998)
34. S. Nazaré, R. Davis, A review of fire blocking technologies for soft furnishings. Fire Sci. Rev. **1**(1), 1 (2012)
35. M. Ravey, E.M. Pearce, Flexible polyurethane foam I. thermal decomposition of a polyether-based, water-blown commercial type of flexible polyurethane foam. J. Appl. Polym. Sci. **63**(1), 47–74 (1997)
36. E. Weil, S. Levchik, Flame retardants in commercial use or development for textiles. J. Fire Sci. **26**, 243–281 (2008)
37. Q. Qiu, M. Kumosa, Corrosion of E-glass fibers in acidic environments. Compos. Sci. Technol. **57**, 497–507 (1997)
38. X. Chen, W. Wang, S. Li, C. Jiao, Fire safety improvement of paraaramid fiber in thermoplastic polyurethane elastomer. J. Hazard. Mater. **324**, 789–796 (2017)
39. S. Heidari, A. Paren, P. Nousiainen, The mechanism of fire resistance in viscose/silicic acid hybrid fibres. J. Soc. Dyers Colour. **109**(7–8), 261–263 (1993)
40. T.-H. Ko, Characterization of PAN-based nonburning (nonflammable) fibers. J. Appl. Polym. Sci. **47**(4), 707–715 (1993)
41. ASTM D737–18 Standard Test Method for Air Permeability of Textile Fabrics (2018)
42. J.S. Fritz, Ion chromatography. Anal. Chem. **59**(4), 335–344 (1987)
43. R.B. Bradstrut, Kjeldahl method for organic nitrogen. Anal. Chem. **26**(1), 185–187 (1954)
44. ASTM. E1479–16 Standard Practice for Describing and Specifying Inductively Coupled Plasma Atomic Emission Spectrometers (2016)
45. B. Beckhoff, B. Kanngieber, N. Langhoff, R. Wedell, H. Wolff, *Handbook of Practical X-Ray Fluorescence Analysis* (Springer, Berlin, Germany, 2006)
46. O.D. Sparkman, Z. Penton, F. Kitson, *Gas Chromatography and Mass Spectrometry: A Practical Guide*, 2nd edn. (Academic Press, Cambridge, MA, 2011)
47. ASTM. C1875–18 Standard Practice for Determination of Major and Minor Elements in Aqueous Pore Solutions of Cementitious Pastes by Inductively Coupled Plasma Optical Emission Spectroscopy (ICP-OES) (2018)
48. M. Petreas, R. Gill, S. Takaku-Pugh et al., Rapid methodology to screen flame retardants in upholstered furniture for compliance with new California labeling law (SB 1019). Chemosphere **152**, 353–359 (2016)

49. H.M. Stapleton, S. Klosterhaus, A. Keller et al., Identification of flame retardants in polyurethane foam collected from baby products. Environ. Sci. Technol. **45**, 5323–5331 (2011)
50. C.-Y. Wang, S.D. Bunday, J.G. Tartar, Ion chromatographic determination of fluorine, chlorine, bromine, and iodine with sequential electrochemical and conductometric detection. Anal. Chem. **55**(9), 1617–1619 (1983)
51. J.F. Colaruotolo, R.S. Eddy, Determination of chlorine, bromine, phosphorus, and sulfur in organic molecules by ion chromatography. Anal. Chem. **49**(6), 884–885 (1997)
52. W.P. Shorrock, O.B. Yale, Inventors; Pilkington PLC, Merseyside, England, assignee. Borosilicate Glass Composition 55 (1993)
53. T. Furukawa, W.B. White, Raman spectroscopic investigation of sodium borosilicate glass structure. J. Mater. Sci. **16**, 2689–2700 (1981)
54. H.P. Hood, M.E. Nordberg, Inventors. Treated Borosilicate Glass (1938)
55. K.K. Shen, R. O'Connor, Flame retardants: borates, in *Plastics Additives: An A-Z Reference*, ed. by G. Pritchard (Springer, Dordrecht, The Netherlands, 1998), pp. 268–276
56. H.D. Brabandere, N. Forsgard, L. Israelsson et al., Screening for organic phosphorus compounds in aquatic sediments by liquid chromatography coupled to ICP-AES and ESI-MS/MS. Anal. Chem. **80**, 6689–6697 (2008)
57. E. Hoh, N.G. Dodder, S.J. Lehotay, K.C. Pangallo, C.M. Reddy, K.A. Maruya, Nontargeted comprehensive two-dimensional gas chromatography/time-of-flight mass spectrometry method and software for inventorying persistent and bioaccumulative contaminants in marine environments. Environ. Sci. Technol. **46**, 8001–8008 (2012)
58. T. Ohlemiller, K.M. Villa, NISTIR 4348 - furniture flammability: Sn investigation of the California bulletin 133 Test. Part 2. Characterization of the ignition source and a comparable gas burner. NIST (1990)
59. F. Rogers, T. Ohlemiller, Smolder characteristics of flexible polyurethane foams. J. Fire Flammability. **11**(1), 32–44 (1980)
60. R.H. Krämer, M. Zammarano, G.T. Linteris, U.W. Gedde, J.W. Gilman, Heat release and structural collapse of flexible polyurethane foam. Polym. Degrad. Stab. **95**(6), 1115–1122 (2010)
61. G. Rein, *Smoldering combustion. SFPE Handbook of Fire Protection Engineering* (Springer, New York, NY, 2016), pp. 581–603
62. X. Zhao, Y.-T.T. Liao, M.C. Johnston, T'J.S. Ien, P.V. Ferkul, S.L. Olson, Concurrent flame growth, spread, and quenching over composite fabric samples in low speed purely forced flow in microgravity. Proc. Combust. Inst. **36**(2), 2971–2978 (2017)
63. J. Sherratt, D.D. Drysdale, The effect of the melt-flow process on the fire behaviour of thermoplastics. Paper presented at: Interflam 2001. Edinburgh (2001)
64. I. Kim, A.L. Thompson, S.C. Kim et al., Demonstration of an all-in-one solution for fire safe upholstery furniture: a Benign backcoating for smoldering and flame-resistant cover fabrics. Fire Mater. **46**(4), 677–693 (2022)
65. R.A. Bryant, M.F. Bundy, The NIST 20 MW calorimetry measurement system for large-fire research. NIST Technical Note 2077 (2019)
66. B.N. Taylor, C.E. Kuyatt, *Guidelines for Evaluating and Expressing the Uncertainty of NIST measurement results. NIST Technical Note*, vol. 1297 (1994)
67. M.C. Bruns, Estimating the flashover probability of residential fires using Monte Carlo simulations of the MQH correlation. Fire Technol. **54**(1), 187–210 (2018)
68. B. Sundstrom, Combustion behavior of upholstered furniture. Important findings, practical use, and implications. Fire Mater. **45**, 97–113 (2020)
69. H. Denize, *The Combustion Behaviour of Upholstered Furniture Materials in New Zealand*. Civil Engineering, University of Canterbury ISSN 1173–5996 (2000)
70. S. Mehta, *Upholstered Furniture Full Scale Chair Tests-Open Flame Ignition Results and Analysis* (Consumer Product Safety Commission, 2012)
71. J. Sherratt, D. Drysdale, The effect of the melt-flow process on the fire behavior of thermoplastics, in *INTERFLAM* (2001)

72. M. Zammarano, S. Matko, W.M. Pitts, D.M. Fox, R.D. Davis, Towards a reference polyurethane foam and bench scale test for assessing smoldering in upholstered furniture. Polym. Degrad. Stab. **106**, 97–107 (2014)
73. D.A. Purser, J.D. McAllister, Assessment of hazards to occupants from smoke, toxic gases and heat. *SFPE Handbook of Fire Protection Engineering*, 5th edn. (Springer, New York, 2016), pp. 2308–2428
74. F.F. Chen, C. Fleischmann, *Radiant Ignition of New Zealand Upholstered Furniture Composites* (University of Canterbury, Christchurch, New Zealand, 2001)
75. SFPE, *Engineering Guide: Piloted Ignition of Solid Materials Under Radiant Exposure* (Society of Fire Protection Engineers, Gaithersburg, MD, 2002)
76. T.J. Ohlemiller, R.G. Gann, Estimating reduced fire risk resulting from an improved mattress flammability standard. NIST Tech. Note **1446**, 80 (2002)
77. R.H. Kramer, M. Zammarano, G.T. Linteris, U.W. Gedde, J.W. Gilman, Heat release and structural collapse of flexible polyurethane foam. Polym. Degrad. Stab. **95**, 1115–1122 (2010)
78. V. Babrauskas, Pillow burning rates. Fire Saf. J. **8**(3), 199–200 (1985)
79. H.E. Mitler, K-M. Tu, Effect of ignition location on heat release rate of burning upholstered furniture. Paper presented at: Annual Conference on Fire Research: Book of Abstracts (1994)
80. M.C. Bruns, Predicting the effects of barrier fabrics on residential upholstered furniture fire hazard. NIST Tech. Note 1920 (2016)
81. NFPA: NFPA 1710, *Standard for the Organization and Deployment of fire Suppression Operations, Emergency Medical Operations, and Special Operations to the Public by Career Fire Departments* (National Fire Protection Association, 2010)
82. NFPA, *NFPA 1720, Standard for the Organization and Deployment of Fire Suppression Operations, Emergency Medical Operations, and Special Operations to the Public by Volunteer Fire Departments* (2010)
83. T. Graham, G.M. Makhviladze, J.P. Roberts, On the theory of flashover development. Fire Saf. J. **25**(3), 229–259 (1995)
84. ISO 13571, Life-threatening components of fire—guidelines for the estimation of time to compromised tenability in fires (2012)
85. S.T. McKenna, R. Birtles, K. Dickens, R.G. Walker, M.J. Spearpoint, A.A. Stec, T.R. Hull, Flame retardants in UK furniture increase smoke toxicity more than they reduce fire growth rate. Chemosphere **196**, 429–439 (2018)
86. V. Babrauskas, B.C. Levin, R.G. Gann, M. Paabo, R.H. Harris, R.D. Peacock, S. Yusa, Toxic potency measurement for fire hazard analysis. Fire Technol. **28**(2), 163–167 (1992)
87. L.Y. Cooper, A concept for estimating available safe egress time in fires. Fire Saf. J. **5**(2), 135–144 (1983)